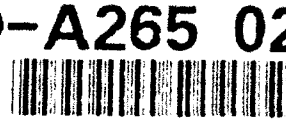

NUSC Technical Report 8739
14 June 1990

A Test Fixture for Detecting the Presence of Water in Buoyant Cables

David Rodriguez
Submarine Electromagnetic Systems Department

Naval Underwater Systems Center
New London, Connecticut / Newport, Rhode Island

Preface

This work was conducted under NUSC Project No. A55400; Principal Investigator C.E. Odams. The NUSC Program Manager is A.R. Susi, Code 34292. The sponsoring activity is SPAWAR PMW-153-2; Project Manager Michael Sheehan.

The technical reviewer for this report was Kurt F. Hafner.

Acknowledgements

The author would like to thank the following people: Dr. John P. Casey and Mr. Kurt F. Hafner for their helpful criticisms and suggestions; Messrs. Walter Roderick, David L. Culbertson and Charles D. Spellman of the Antenna Systems Branch, along with Messrs. Craig L. Flynn, Eric von Winkle and Phillip Watrous of the Pressure Lab for their assistance in the measurements, and Mr. Lucius D. Stark of the Mechanical Design Branch for preparing the exploded view of the device, Fig. A.1 (Appendix A).

Reviewed and Approved: 14 June 1990

D. M. Viccione
Head, Submarine Electromagnetic
Systems Department

Mr. Rodriguez is located at the New London Laboratory,
Naval Underwater Systems Center,
New London, Connecticut 06320

REPORT DOCUMENTATION PAGE

Form Approved
OMB No 0704-0188

1. AGENCY USE ONLY (Leave blank)	2. REPORT DATE	3. REPORT TYPE AND DATES COVERED
	14 June 1990	Final

4. TITLE AND SUBTITLE
A test fixture for detecting the presence of water in buoyant cables.

5. FUNDING NUMBERS
A55400

6. AUTHOR(S)
David Rodriguez

7. PERFORMING ORGANIZATION NAME(S) AND ADDRESS(ES)
New London Laboratory
New London, CT 06320-5594

8. PERFORMING ORGANIZATION REPORT NUMBER
TR 8739

9. SPONSORING/MONITORING AGENCY NAME(S) AND ADDRESS(ES)
Space and Naval Warfare
PMW 153-2
Washington, DC

10. SPONSORING/MONITORING AGENCY REPORT NUMBER

11. SUPPLEMENTARY NOTES

12a. DISTRIBUTION/AVAILABILITY STATEMENT
Approved for public release; distribution unlimited.

12b. DISTRIBUTION CODE

13. ABSTRACT (Maximum 200 words)

A simple low-frequency technique for determining the presence of water or moisture in buoyant cables has been developed. It is used primarily a diagnostic tool for rejecting cables containing traces of sea water.

The method makes use of test fixture in the form of a curved-plate capacitor. The plate configuration of the capacitor was designed in such a manner that its sensitivity to low levels of moisture (less than 0.1 ounce per foot) is accompanied by large percentage increases in capacitance from the nominal dry value. Typical increases in capacitance for such levels have been observed in the range of 12% to 25%, with fully saturated cables exhibiting maximum changes as large as 70%. A mathematical expression for volume of water present in a cable as a function of the percentage increase in capacitance was derived and has been shown to agree with experimental data.

14. SUBJECT TERMS		15. NUMBER OF PAGES
TEXT FIXTURE	HYDROSTATIC TEST	
CAPACITANCE	LOW FREQUENCY	16. PRICE CODE
BUOYANT CABLE		

17. SECURITY CLASSIFICATION OF REPORT	18. SECURITY CLASSIFICATION OF THIS PAGE	19. SECURITY CLASSIFICATION OF ABSTRACT	20. LIMITATION OF ABSTRACT
UNCLASSIFIED	UNCLASSIFIED	UNCLASSIFIED	UNLIMITED

DISCLAIMER NOTICE

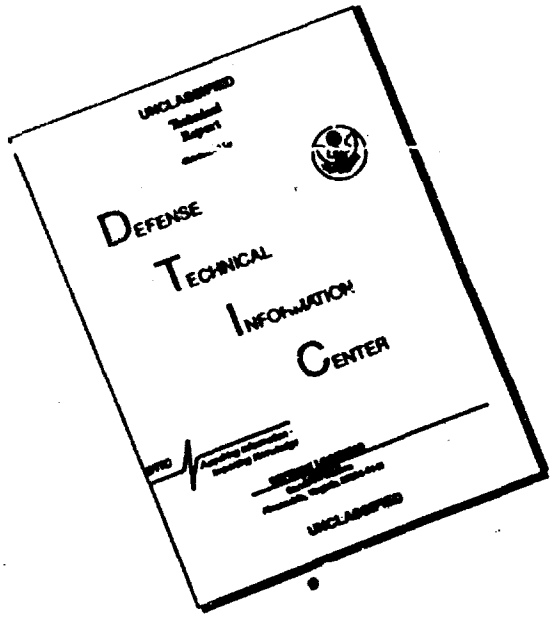

THIS DOCUMENT IS BEST QUALITY AVAILABLE. THE COPY FURNISHED TO DTIC CONTAINED A SIGNIFICANT NUMBER OF PAGES WHICH DO NOT REPRODUCE LEGIBLY.

TABLE OF CONTENTS

LIST OF ILLUSTRATIONS

LIST OF ILLUSTRATIONS (Cont'd)

REVERSE BLANK

1. INTRODUCTION

This paper explores the design and implementation of a simple test fixture that indicates the presence of water or moisture inside buoyant cables. The principle employed in the development of the test fixture could be applied to any type of cable. The test fixture actually built was designed to only accommodate cables with an outer diameter of 0.65 inch. It was the leakage of water in NUSC-C-279/3-11 cable (hereafter referred to as type 3-11 cable) that motivated the development of the test fixture.

The migration of water in buoyant cables is caused in part by small cracks or holes on the outer jacket and/or by an incomplete filling with a water blocking compound (Vistanex™ and Eccogel ™). These conditions, in the presence of the large hydrostatic pressure exerted by the sea, cause the migration of water in the cable. The flooding, if left unchecked, may damage the electrical connections and antenna - deployment mechanisms by causing short circuits and forming rust.

The determination of water presence, as indicated by the test fixture, is made in terms of capacitance. Since the complex relative permittivity of water (fresh or sea) has a large magnitude, changes in capacitance from the dry cable state can be readily observed. The amount of water can then be found by means of a graph relating the observed capacitance to a quantity of water, or by an algebraic expression.

The details pertaining to the year that the flooding problem arose are not precisely known. What *is* known, however, is that the severity (as noted by the frequency of failure reports received by NUSC), escalated to the point where serious attention to its nature and isolation was paid in the late fall of 1985. The problem was examined by repeated testing of the cable in accordance with NUSC-C-342/4141-279 specifications. The cable under consideration was the RF cable designated as type 3-11. The construction of the cable (shown in Fig. 1), caused most of the trapped water to be concentrated between the outer braid of the coaxial line and the foam fillers, although signs of flooding in the plastic sheath enveloping the twisted pair and portions of the space inside the coaxial line have been observed.

2. TEST FIXTURE DEVELOPMENT

2.1. General.

The development of an instrument to measure the moisture content in a suspect cable grew out of a 120-hour First-Article test conducted at NUSC on a sample of type 3-11 cable. In this test, 750 feet of cable was installed in a pressure vessel and subjected to 450 pounds per cubic inch gauge (PSIG). A short length of the cable (3 to 4 feet) was exposed to the atmosphere through an opening in the vessel, creating a difference in pressure. Figure 2 shows the test setup.

In order to monitor the degree of flooding, the conductors of the twisted pair (Fig. 1) were connected together, forming an extended conducting element. With the coaxial braid forming the remaining conductor, an elementary capacitor was made. An impedance analyzer was used to measure the capacitance between the combined conductors of the twisted pair and the shield of the coaxial cable. The capacitance variation with time is plotted in Fig. 3. The cable end exposed to the atmosphere began to leak after 164 hours had elapsed (the test was extended to accommodate this event), at a rate of 6.3 cubic inches per hour. Note that the leakage of water resulted in an increase in capacitance.

The procedure just mentioned provided the motivation for an alternate means of detecting water without physically cutting the cable. A noninvasive measurement of water penetration was considered important, since cutting the cable would render the cable useless for further service. Such a means would be beneficial for cables containing minute amounts of water (less than 0.1 ounce per foot). These amounts would not seriously affect the cable's buoyancy or its electrical characteristics, remaining operational.

2.2. The curved-plate capacitor.

The detection of water, as explained in § 2.1, utilized some of the conducting elements in the cable to form a capacitor. The change in capacitance between conductors within the cable could be used to identify specific regions along a sample length in which water was present. Ambiguities with regard to location and quantity of water existed.

An alternative to measuring the capacitance between conductors within the cable was realized by use of a conducting element pair in the form of thin curved strips conforming to the cable's outer jacket. The capacitance between curved strips could be used to determine the presence of water within the cable. The pair of curved metal strips will be referred to as the capacitor. The concept was tested with the model shown in Fig. 4, using the same hydrostatic test setup of Fig. 2. The variation in capacitance with time as water was forced through the cable is shown in Fig. 5.

2.3. Low-frequency electromagnetic shielding.

The use of a metal shield to house the capacitor was found to provide isolation from electrical noise. Measurements made without the shell at a frequency of 20 kHz (in earlier tests), were difficult to interpret. The instabilities in the capacitance readings due to the low frequency noise were reduced by raising the measurement frequency to 50 kHz. At this frequency, however, problems due to the handling of the device were most pronounced. Figure 6 shows the shield, made out of copper foil and plastic. A short piece of copper braid, connected to one end of the shield, allowed it to be placed at ground potential. Tests with the capacitor / shield combination were made to assess the performance of the complete assembly; the results are plotted in Fig. 7.

2.4. The location of water.

Tests described thus far to determine the device's effectiveness in detecting water were done with the device fixed at a specific location along the cable's length, using time as a frame of reference. In practice, it is desired to determine the extent of flooding as a function of position along a sample length. Figure 8 is a plot of the variation of capacitance with position, for a partially flooded cable. To make an accurate estimate of the degree of flooding, it is necessary to first establish a base-line capacitance measurement on a dry sample. This is done in order to compare both wet and dry readings. In the present example, a base-line capacitance of 19.4 ± 0.7 pF was observed throughout the entire sample length ($\approx$ 36 feet).

3. TEST FIXTURE DESIGN

3.1. Test fixture design considerations.

The tests described in the previous section were performed in order to evaluate the usefulness of the proposed moisture detecting test fixture. The remaining work to be done was to improve the device. Toward this end, the areas considered were:

Capacitor plate design. The device's ability to detect minute traces of water is related to the size of the gaps on the plates (refer to Fig. 4). A test to determine the appropriate gap size required to increase the sensivity to low levels of moisture had to be performed.

Shield design. The proper design of a low-frequency shield that offered a degree of immunity to electrical noise was needed. Moreover, the need for ruggedness was of considerable importance. Lastly, a mechanism for keeping the cable sample straight during testing was desirable. This feature allowed for uniformity in testing, and was achieved by means of springs, pulleys or rollers.

Capacitance/moisture content correspondence. Calibration of the device in terms of moisture content was needed. The presence of water has been demonstrated to cause an increase in capacitance, but a relationship between the quantity of water causing an increase from a dry nominal (capacitance) value was absent. The quantity of water responsible for the change in relative permittivity is then found by the method discussed in § 4.3.

3.2. Capacitor plate design. Capacitance per unit length.

The capacitance per unit length of two curved cylindrical plates about a solid cylinder as shown in Fig. 9(a) can be computed from eq. (1) under the assumption that the plates are infinitesmally thin. The result is plotted in Fig. 9(b). The exact expression for this quantity, which accounts for electric field fringing, is given by [1]:

$$C = 2\,\varepsilon\,\frac{K(k')}{K(k)} \tag{1}$$

where

C = the capacitance per unit length

ε = the permittivity of the medium surrounding the capacitor

and K = the complete elliptic integral of the first kind, of modulus k and k' (Appendix B). The moduli are functions of the capacitor's cross-sectional dimensions.

3.2.1. Plate thickness correction.

The capacitance per unit length given by eq. (1) was derived under the assumption that the plate thickness is vanishingly small. For the practical case where a capacitor with a plate thickness "t" is given, a correction term must be added. Figure 11 is a plot of the correction term, based on work done by Bochenek [2] and Hilberg [3] . A simple approximation for a capacitor with $t/D \geq 0.05$ and $s/D \leq 0.25$ is given by [4]:

$$\Delta C \approx \varepsilon \frac{\ln\left\{1 + 2\left(\frac{t}{D}\right)\right\}}{\sin^{-1}\left\{\frac{\left(\frac{s}{D}\right)}{\left\{1 + 2\left(\frac{t}{D}\right)\right\}}\right\}} \tag{2}$$

where D is the inner diameter of the capacitor, and is accurate to within 10 percent. The resulting expression for the total capacitance per unit length is then:

$$C_{total} = C + \Delta C \tag{3}$$

3.2.2. Plate sensitivity.

The resulting change in capacitance, due to a change in permittivity, is referred to as plate sensitivity, defined by [5]:

$$S_{plate} = \frac{\partial C}{\partial \varepsilon} \tag{4}$$

where ε is the *effective* relative permittivity of the medium in which the capacitor is immersed and C is C_{total}, defined in eq. (3). The plate-gap distance, s, is found (holding dimensions d and D constant) so as to make eq. (4) as large as possible. The gap distance is determined through a combination of calculation and experiment.

3.3. Low-frequency electromagnetic shield.

The design of a shield required to reduce electrical interference at the instrument's operating frequency, 50 kHz, was chosen to have a cylindrical shape. Unlike the earlier version (Fig. 5), the metallic wall thickness and outer diameter was increased to yield a higher degree of shielding. Shenfeld [6] gives an expression for the shielding effectiveness of a non-magnetic ($\mu_r = 1$) cylinder as:

$$\frac{H_o}{H_i} = \cosh(\gamma d) + \left\{\frac{\gamma a}{2}\right\} \sinh(\gamma d) \qquad (5)$$

where

H_o = amplitude of the incident magnetic intensity (amperes/meter)

H_i = amplitude of the magnetic field intensity internal to the cylinder (amperes/meter)

a = outer radius of the cylinder (meters)

d = wall thickness (meters)

γ = the wave propagation constant in the cylinder material (Neper/meter) = $\sqrt{j\,\omega\,\mu_o\,\sigma}$

The symbols j, ω, μ_o and σ denote the complex number ($j = \sqrt{-1}$), angular frequency ($2\pi f$), permeability of free-space ($4\pi \times 10^{-7}$ H/m) and electrical conductivity (S/m), respectively. Figure 11 shows the variation in shielding effectiveness (expressed in dB) for different cylindrical sizes and materials, described by the parameter P and material skin-depth δ, as:

$$P = \frac{a}{2d} \quad \text{and} \quad \delta = \sqrt{\frac{2}{\omega\,\mu_o\,\sigma}}$$

3.4. Capacitance/moisture content.

An expression for determining an effective overall permittivity (ε^*) from the constituent parts of the material within the curved plate capacitor is derived in Appendix D and presented in eq. (6) below [7,8]:

$$\ln(\varepsilon^*) = \sum_{i=1}^{N} \vartheta_i \ln(\varepsilon_i) \tag{6}$$

where

ϑ_i = the i^{th} fraction of the total volume in a substance with a relative permittivity of ε_i

N = the number of elements constituting the substance

and

$$\sum_{i=1}^{N} \vartheta_i = 1$$

In the analysis, the increase in capacitance due to the presence of water is found in terms of the resultant permittivity.

4. DESIGN SUMMARY

4.1. Capacitor plate design for high sensitivity.

Experiments performed to determine an appropriate plate-gap distance for high sensitivity, indicated that the use of small gaps were necessary (see Fig. 12). A suitable choice of the gap to diameter ratio (s/D) was at the designer's discretion, dictated primarily by mechanical limits (i.e., an adherence to construction tolerances). Therefore, the final choice was as follows:

i) plate gap (s): 0.2 inch
ii) plate inner diameter (D): 0.7 inch
iii) plate length (L): 24 inches
iv) plate thickness (t): 0.025 inch
v) material: brass
vi) computed capacitance ≈ 22 pF ($\varepsilon_r = 1$, d ≈ 0.18 inch)

4.2. Low-frequency electromagnetic shield.

For the design of the electromagnetic shield, Fig. 11 was used. The plot indicates that the shielding effectiveness varies directly with the cylinder's diameter and wall thickness. An increase in wall thickness, however, results in a heavier shield, thereby limiting the device's portability. Therefore, the diameter of the shield was considered over the wall thickness, with the following dimensions:

i) shield outer diameter: 3 inches
ii) shield length: 26 inches
iii) wall thickness: 1/8 inch
iv) material: brass

Using the dimensions given above in eq. (5), the shielding effectiveness as a function of frequency is plotted in Fig. 13, where at 50 kHz it is seen to have a value of 43 dB (the copper shield used in the earlier experiments had a shielding effectiveness of 26 dB at the same frequency).

To enhance the mechanical performance of the device, guide rollers were designed to provide tension so that the cable under test would remain straight. The degree of tension applied to the cable is adjustable by means of a lever-arm assembly. Figures 14 and 15 show the completed device.

4.3. Capacitance/moisture content correspondence.

The volume of water *per unit length*, V_f, required to raise the dry cable capacitance C_m to a flooded value C_t, as discussed in § 3 and Appendix D, is approximated by:

$$V_f \approx \left[\left(\frac{W_c}{\xi_c \rho_f g}\right) - \pi a^2\right]\left[\frac{\kappa \ln\left(\frac{C_t}{C_m}\right)}{1 - \kappa \ln\left(\frac{C_t}{C_m}\right)}\right], \text{ for } 1 \le \left(\frac{C_t}{C_m}\right) < \sqrt{\frac{\varepsilon_f}{\varepsilon_m}} \qquad (7)$$

where W_c = the weight per unit length of the dry cable ≈ 0.1 lb / ft

ξ_c = the specific gravity of the dry cable ≈ 0.74

ρ_f, g = the density of water and acceleration due to gravity, respectively ($\rho_f g \approx 62.4$ lb / ft^3 in English units)

$$\kappa = \frac{1}{\ln\left(\frac{\varepsilon_f}{\varepsilon_m}\right)}$$

and ε_f = the relative permittivity of water ≈ 80 at 20° C

ε_m = the relative permittivity of the cable material ≈ 1.2 to 2.2

a = radius of the center conductor in the cable ≈ 0.092 in.

Figure 16 is a plot of the variation in water content as a function of the percentage increase in capacitance from the dry state, with experimental data.

4.4. Sensitivity of completed unit.

A check on the sensitivity of the completed device was performed in order to assess its behavior under actual conditions, using the definition given in § 3.5. The test utilized a 50 foot sample of 3-11 cable, and was set up in the manner shown in Fig. 17. With the cable under pressure (450 PSIG), the computer recorded the capacitance displayed on the impedance analyzer as a function of time (the recordings were made at one-second intervals), and was programmed to compute the derivative

$$\Phi(\text{pF/minute}) = \frac{dC}{dt} \qquad (8)$$

which can be related to $\partial C/\partial \varepsilon$. Figure 18 shows the variation of Φ with time, where a peak value of 8.4 pF/minute is noted.

The calculation of $\partial C/\partial \varepsilon$ is made with the aid of the relation:

$$\frac{\partial C}{\partial \varepsilon} = \frac{\partial C}{\partial t} \cdot \frac{\partial t}{\partial \varepsilon} \tag{9}$$

where t is the time taken for water to flow through the cable, and ε is the relative permittivity of the cable material. If the center conductor diameter (d) and capacitor diameter (D) are held constant, eq. (9) is simplified using the approximations below:

$$\frac{\partial C}{\partial t} \approx \frac{dC}{dt} = \Phi \quad , \quad \frac{\partial t}{\partial \varepsilon} \approx \frac{dt}{d\varepsilon} \approx \frac{\Delta t}{\Delta \varepsilon} \tag{10}$$

and

$$\frac{\Delta \varepsilon}{\Delta t}\,(\text{inch per minute}) \approx \frac{(C_{wet} - C_{dry})}{C_{air}} \cdot \frac{L}{\Delta t} \tag{11}$$

where

C_{wet} = the wet cable capacitance

C_{dry} = the dry cable capacitance

C_{air} = the capacitance with the center conductor and air as the dielectric

L = the length of the capacitor plates (24 inches).

Substitution of eqs. (10) and (11) yields an estimate for the device's sensitivity as:

$$S_{plate}(\text{pF/inch}) = \frac{\partial C}{\partial \varepsilon} \approx \frac{\Phi}{(\Delta \varepsilon/\Delta t)} \approx \frac{\Phi\, C_{air}\, \Delta t}{L\,(C_{wet} - C_{dry})} \tag{12}$$

where Δt is the time taken for water to flow through the cable segment enclosed by the capacitor plates (the velocity of water flow in the cable is assumed to be constant). Using the following experimental values:

$$C_{wet} \approx 59.1 \text{ pF} \qquad C_{air} \approx 21.1 \text{ pF}$$
$$C_{dry} \approx 42.8 \text{ pF} \qquad \Delta t \approx 2 \text{ minutes}$$

and $\Phi \approx 8.4$ pF/inch (maximum), substitution into eq. (12) yields $S_{plate} \approx 0.90$ pF/inch. This value is larger than that found in the computed curve given in Fig. 12 (s/D = 0.286, $S_{plate} \approx 0.77$ pF/inch), and can be attributed to the effects of the center conductor(s), shield assembly and the finite length of the plates.

5. TEST FIXTURE OPERATION AND USE

5.1. Instrument description.

For an external view of the instrument, refer to Fig. 14. The sample under test is inserted into port A1 or A2. The cable is held in place vertically by an adjustment of the bolts located behind the lever-pivot assemblies labelled D1 and D2, which tighten opposing rollers about the cables. The upper and lower half-shells of the RF shield assembly (C1 and C2) were designed so that both halves can be separated. This feature is necessary for cases where very long cable samples are tested, enabling the operator to survey a specific location without running the cable completely through. Ports B1 and B2 allow connection from the capacitor plates to an impedance analyzer, where the capacitance is displayed.

5.2. Moisture measurement setup and test.

A simple arrangment for checking a flooded cable is shown in Fig. 19. In this setup, the cable-under-test is fed through the instrument from its storage reel and onto the take-up spool. With the cable fastened to the take-up spool, testing can begin by rotating this spool. Experience with this setup has shown that a cable speed of approximately 5 feet per minute through the instrument is preferreable, when inspecting flooded regions or "pockets" throughout a sample length.

TEST PROCEDURE

a) Dry cable readings. This step requires a careful measurement of dry cables for use as a base line, as mentioned in Section 2.2. A nominal value of 36 pF has been measured with the instrument, with deviation due to a combination of changes in the cable diameter, and specific gravity (ξ_c).

b) Wet cable readings. The same procedure used in (a) above is repeated with the wet cable. Readings for this case vary from 40 to 45 pF (light-to-moderate) and from 45 to 60 pF (moderate-to-extreme).

c) Water content determination. This procedure uses Fig. 16 or eq. (7) to determine the water content in the flooded cable. For the wet and dry readings given, this corresponds to a water-to-cable volume range of 3% to 12% (negligible) and 6% to 22% (negligible-to-light).

5.3. Flooding Chart.

The chart below was prepared to complement the plot in Fig. 16. In it, the percentage changes in capacitance, with the resulting changes in the quantity of water, are listed. This chart can be used as a guide in determining the suitability of the cable for further service.

Capacitance change (%)	Quantity of water		Flood description
	% of cable vol.	fl. oz. per ft.*	
0 - 12	0 - 3	0 - 0.06	Negligible
12 - 25	3 - 6	0.06 - 0.11	Light
25 - 52	6 - 12	0.11 - 0.23	Moderate
52 - 100	12 - 22	0.23 - 0.42	Extreme
> 100	> 22	> 0.42	Severe**

* This quantity is computed using a cable with a volume of 3.43 in^3 / ft. ($W_c \approx 0.1$ lb / ft., $\xi_c \approx 0.74$, $a \approx 0.092$ in.), and a conversion factor of 0.554 in^3 / fl. oz. .

** At this level, possible cable damage due to surface rupture can occur.

6. SUMMARY

This paper focused on the development, design and use of a test fixture for detecting water in buoyant cables. It was shown that the implementation of two thin strips, each bent to a radius equal to that of the cable's, allowed for this determination by means of a change in capacitance.

An examination of the properties of the capacitor plate configuration has led to a mechanical design that would yield a large tangential sensitivity, in the region where the ratio of the plate's gap-to-diameter (s/D) is less than 0.5. Such a plate shape ratio has been found to allow a fine degree of resolution in the detection of moisture. A new mathematical expression has been introduced in this paper linking the water content in a flooded sample (as a percentage of the cable's overall volume), to the percentage increase in capacitance. The expression shows that, in general, a 10% change in capacitance results in an 2.5% increase in the fractional volume of water in the cable.

The use of a metallic shield for electromagnetic isolation has been found to enhance the performance of the capacitor, by providing a shielding effectiveness of 43 dB at the operating frequency, 50 kHz. Finally, a simple procedure for testing cables having water damage has been described. In this procedure, the cable (wound on a reel), is fed through the detector by means of a drive mechanism located near a take-up (empty) reel.

REVERSE BLANK

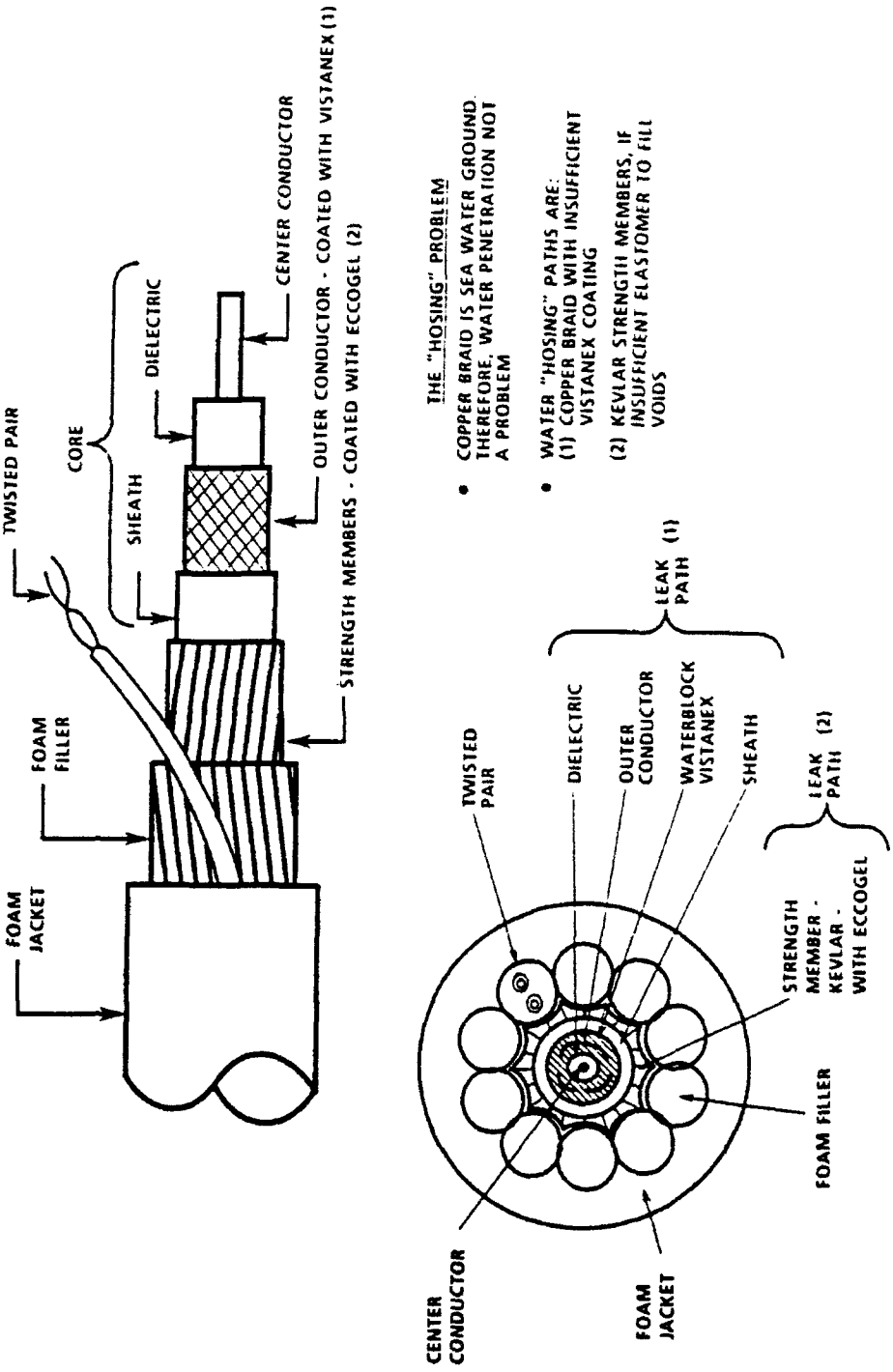

Fig. 1. Potential leak paths.

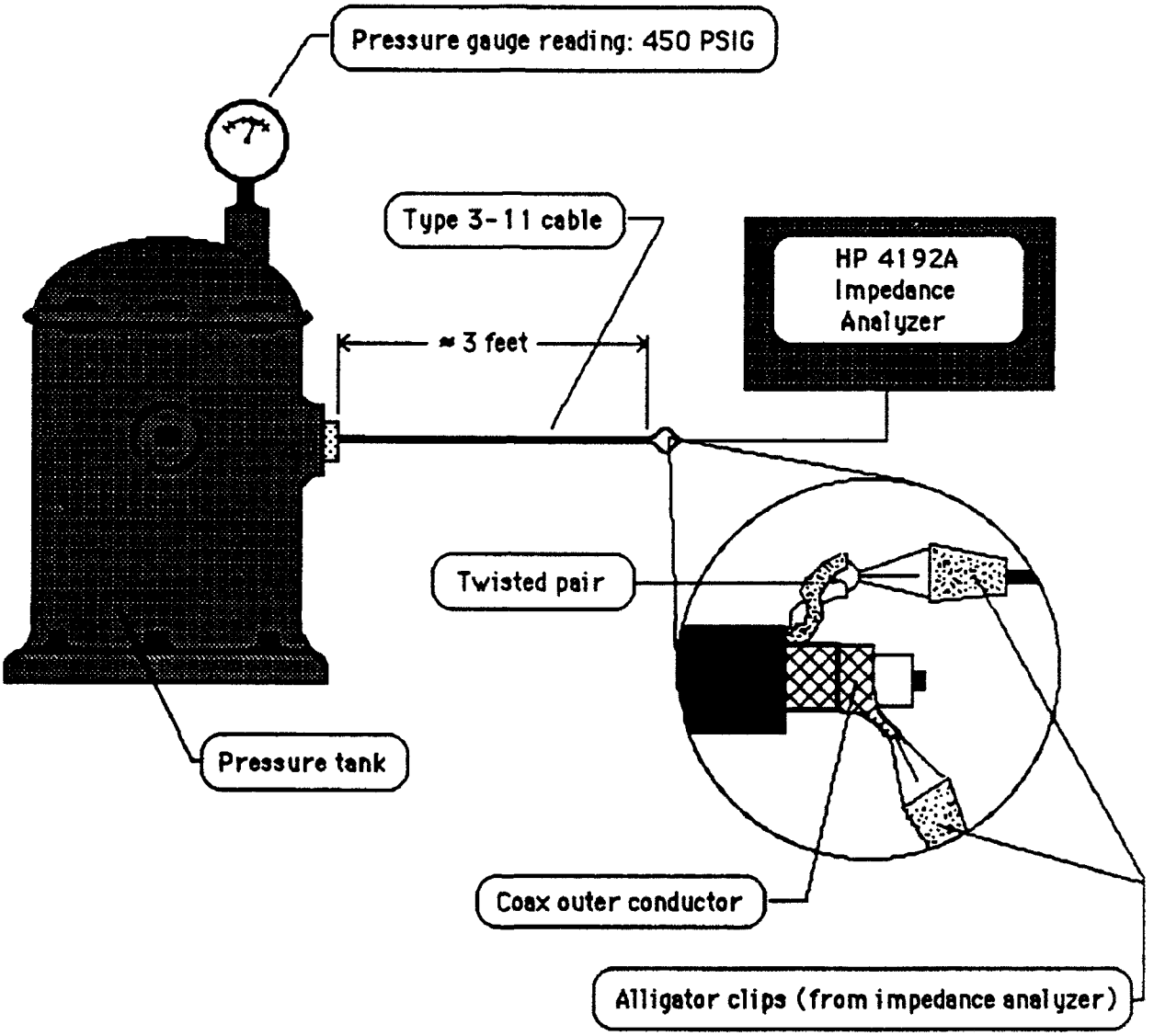

Fig. 2. Initial two-element capacitance test.

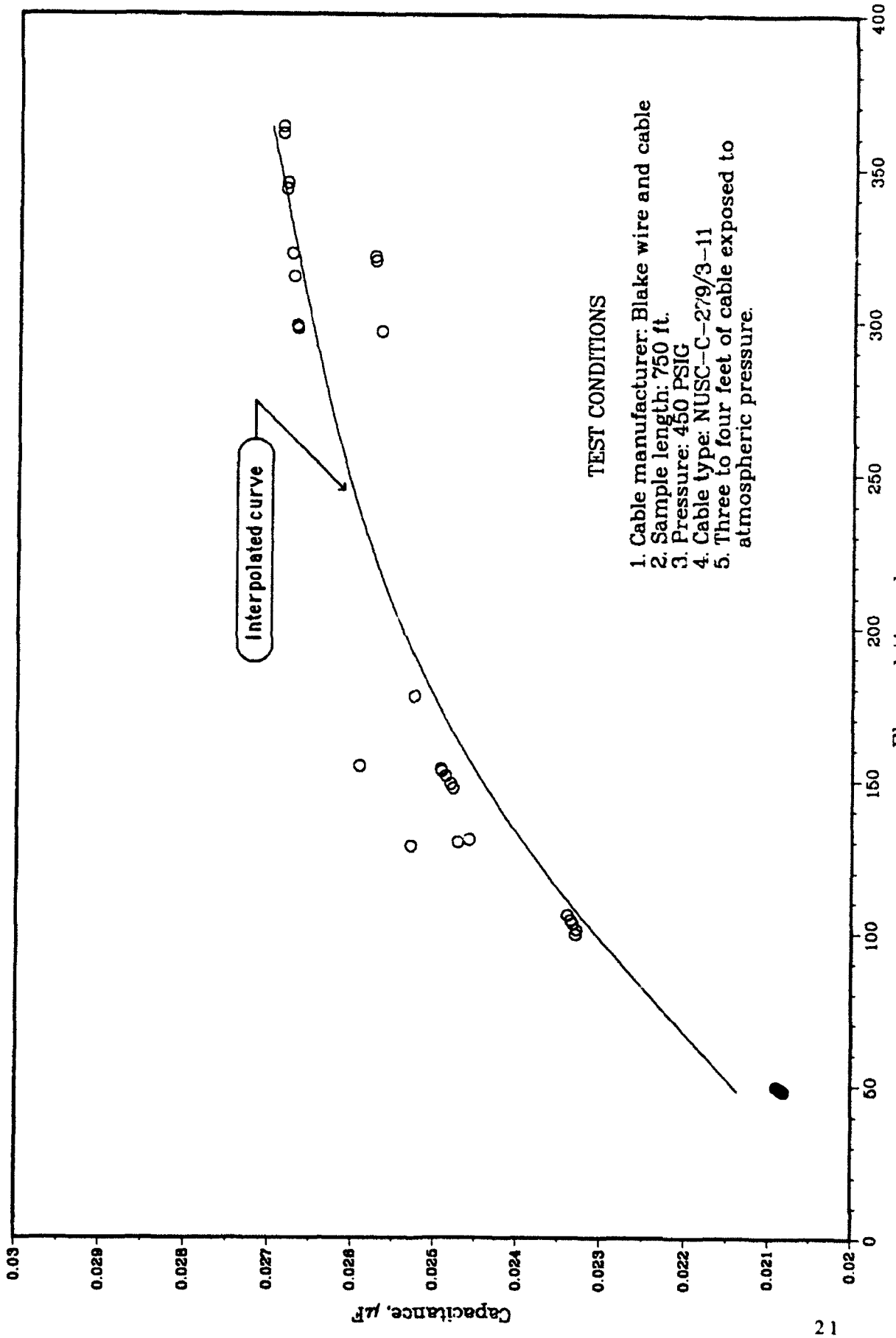

Fig. 3. Capacitance between the combined conductors of the twisted pair and the braid of the coax.

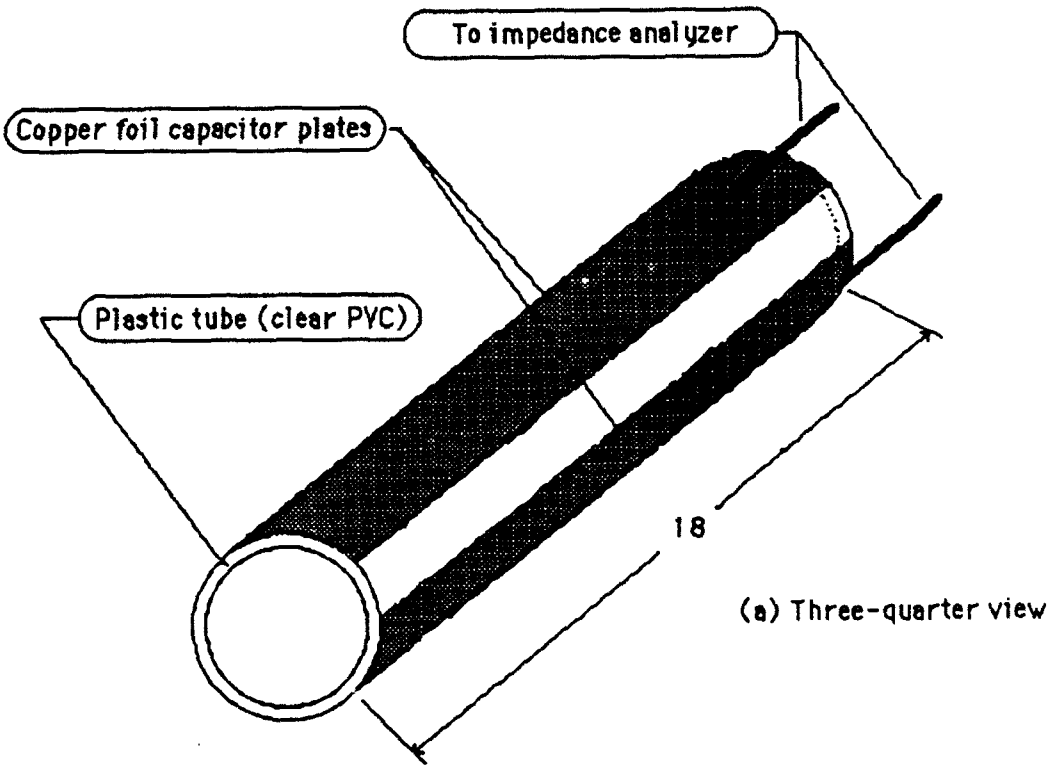

(a) Three-quarter view

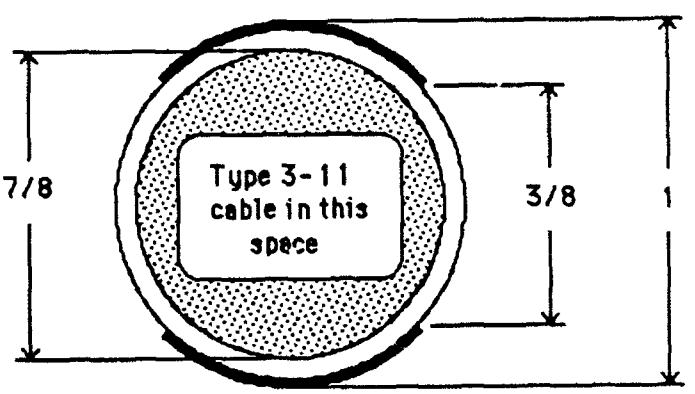

(b) Cross-sectional view

Fig. 4. Curved plate capacitor. Dimensions given are in inches.

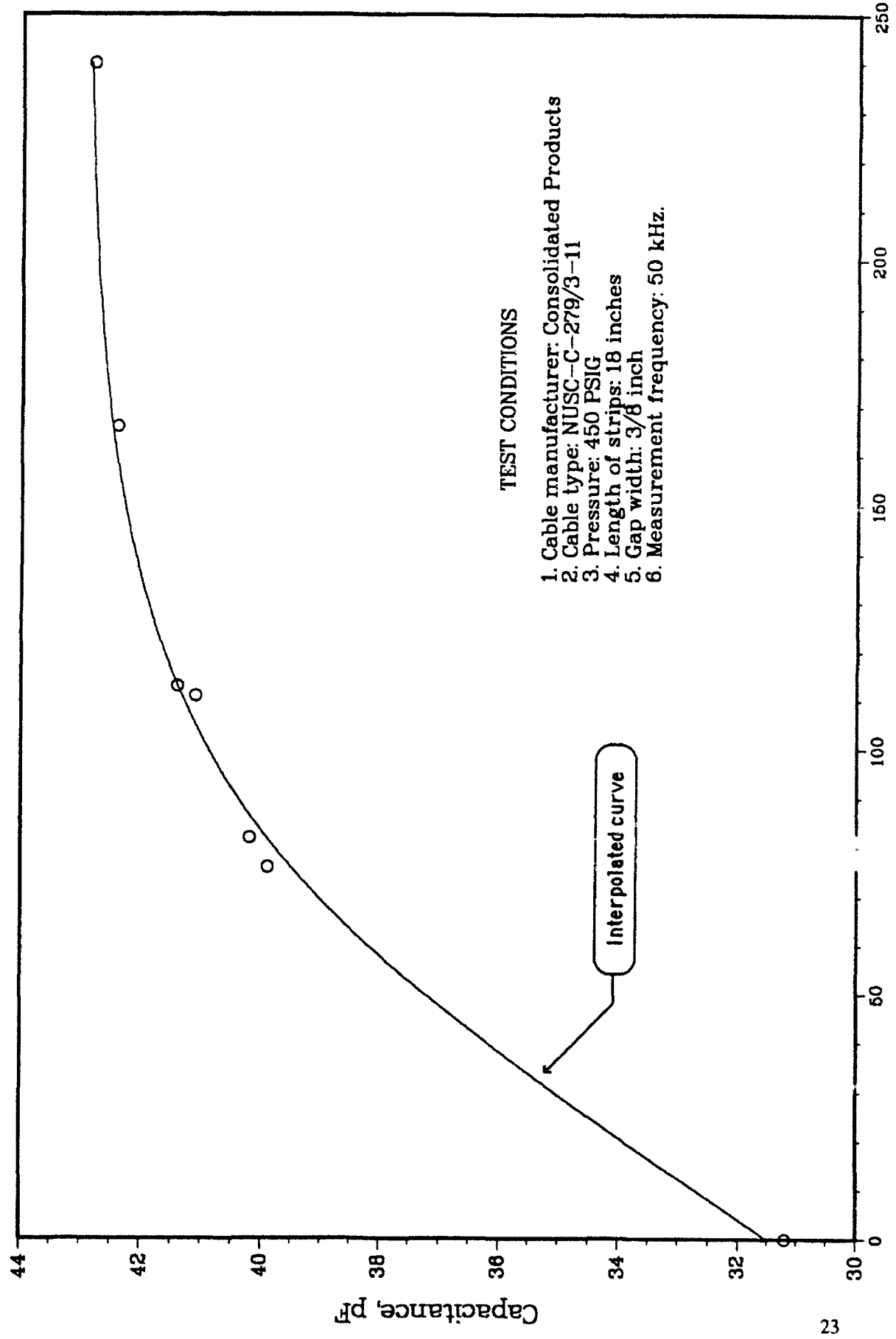

Fig. 5. Capacitance between curved strips exterior to the cable with water migration.

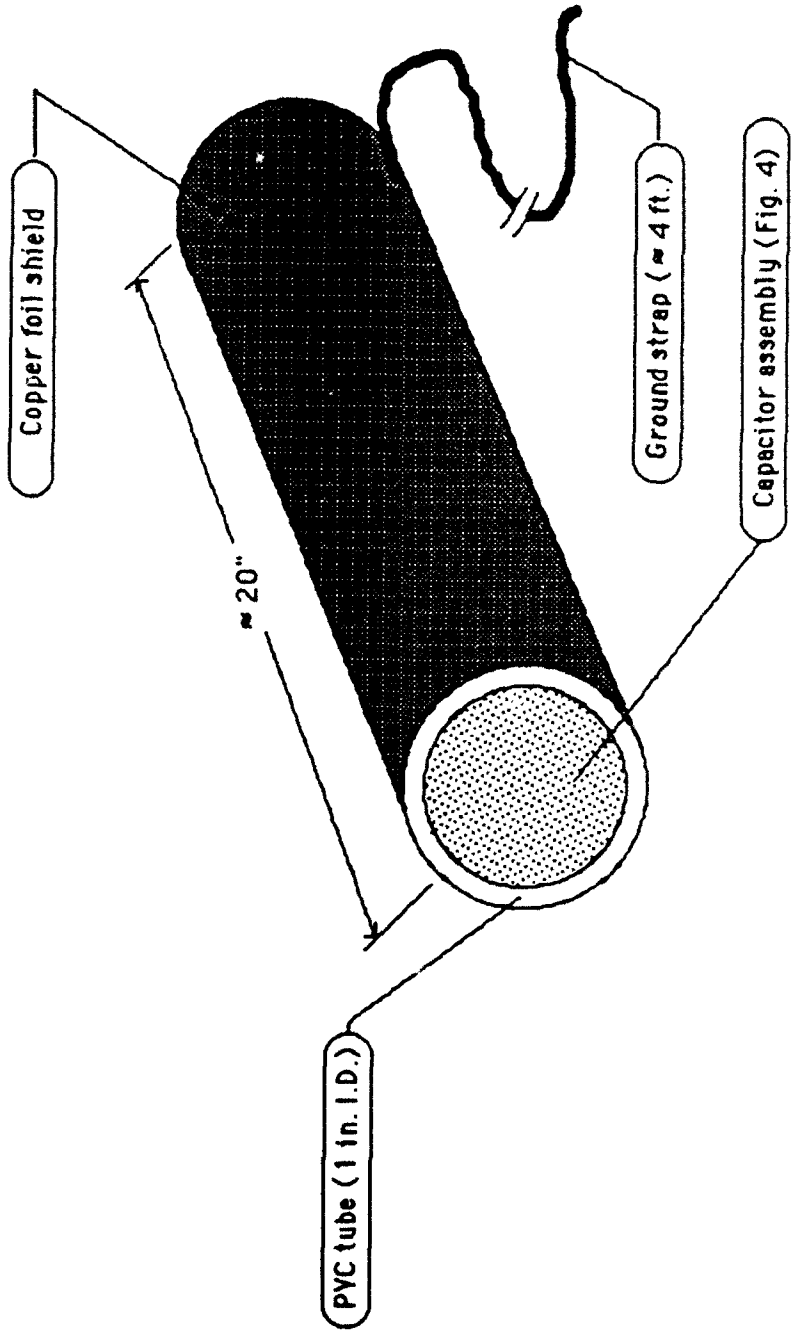

Fig. 6. Low frequency shield.

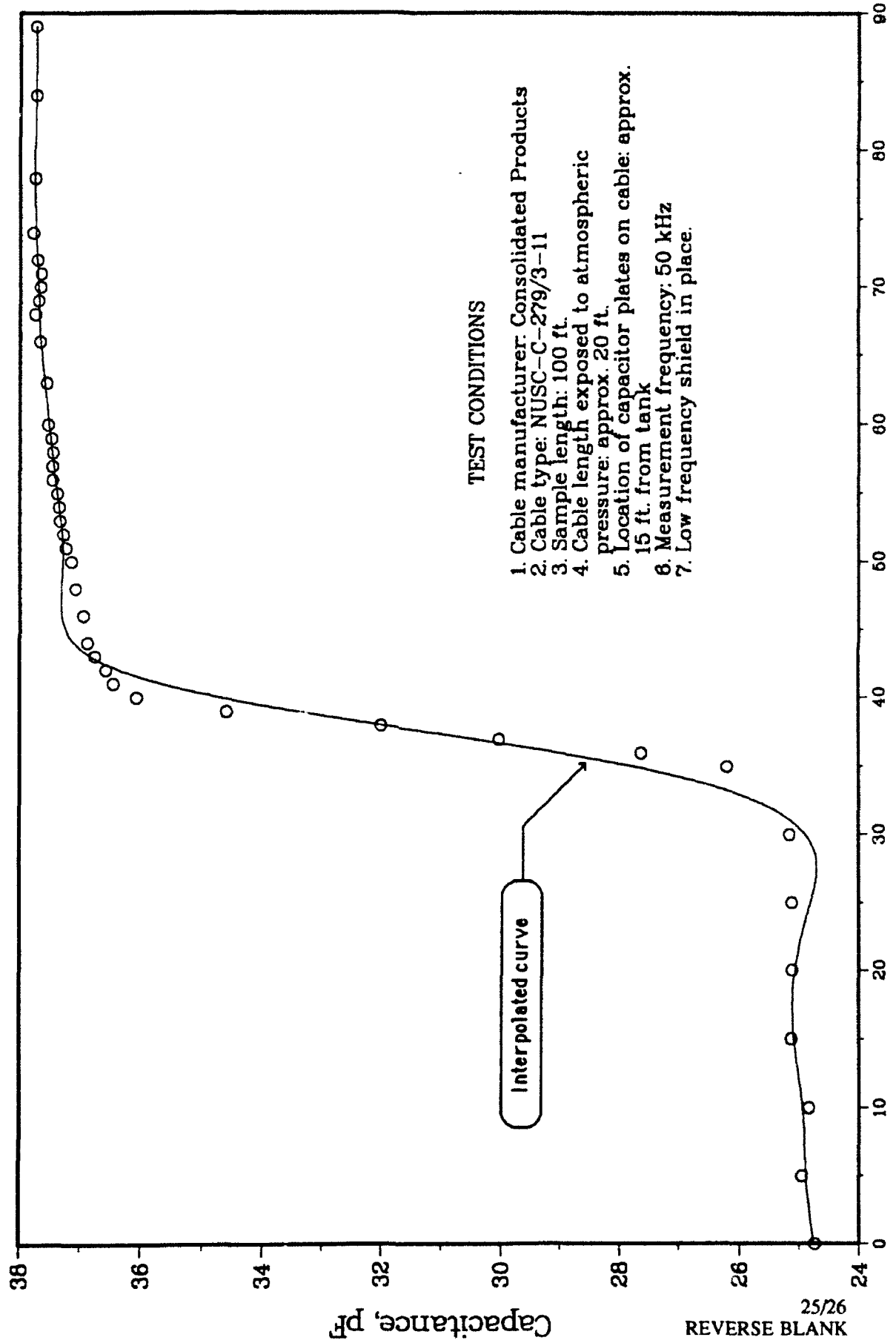

Fig. 7. Capacitance between curved strips with water migration; shield in place.

REVERSE BLANK

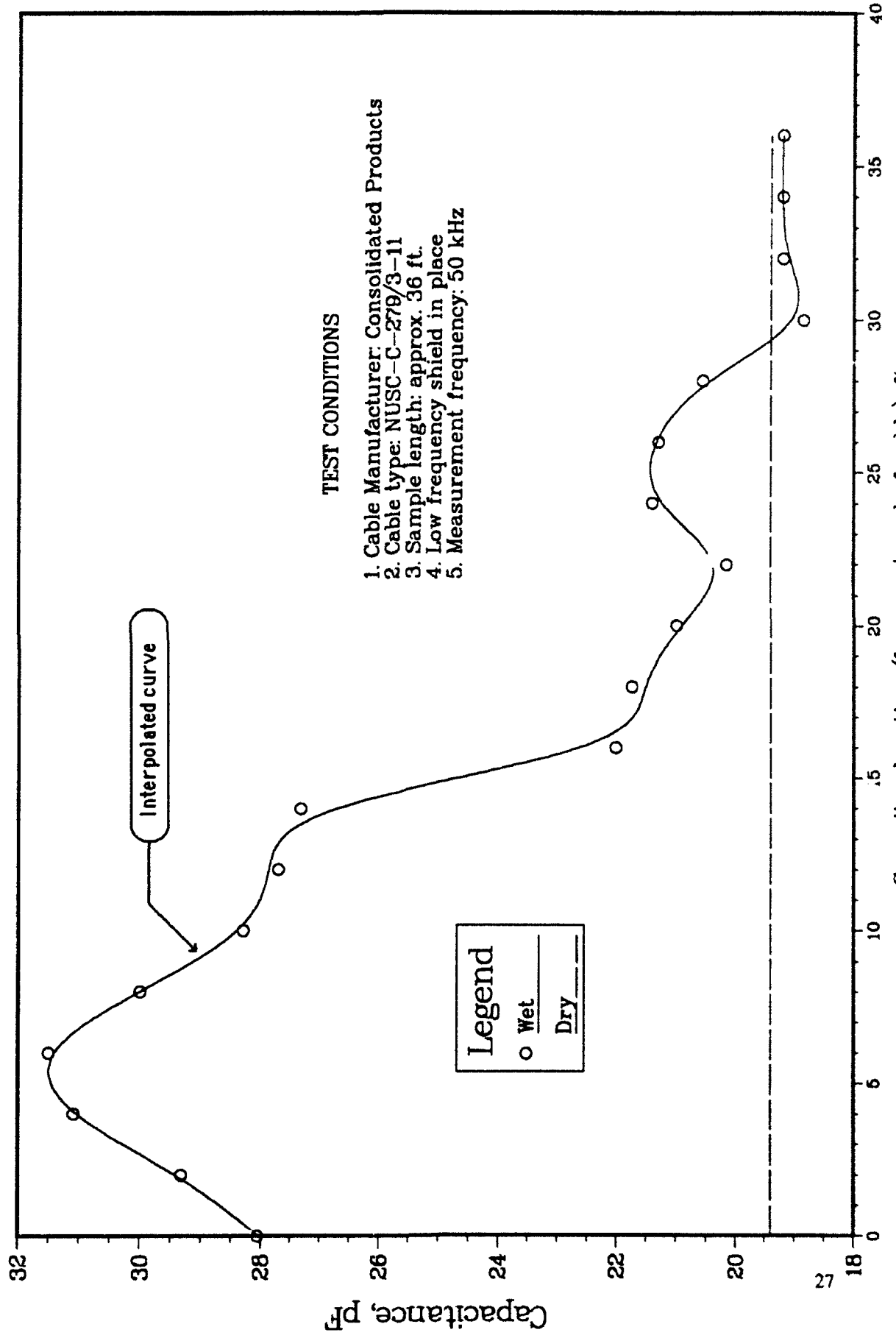

Fig. 8. Capacitance between curved strips; variation with distance

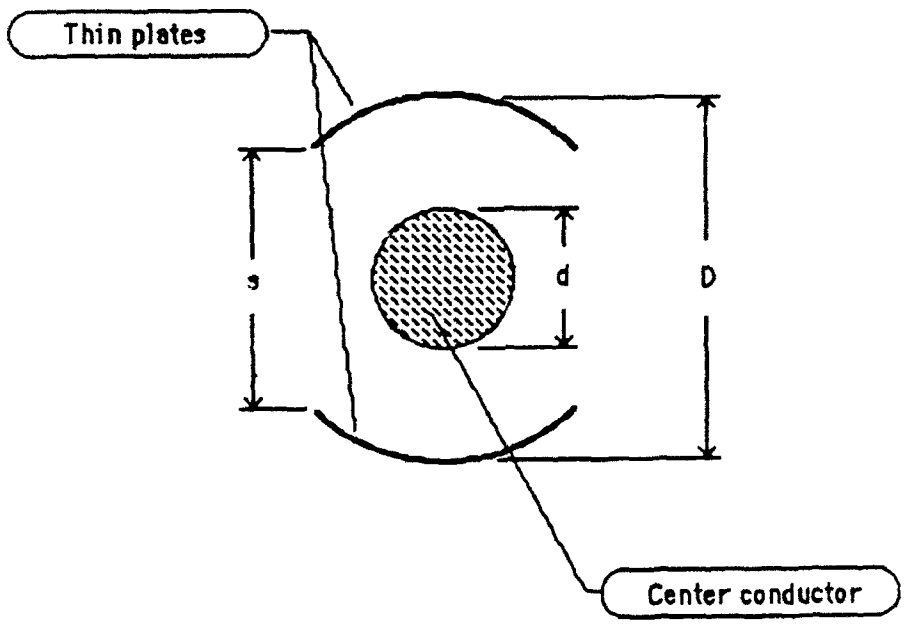

Fig. 9(a). Curved plate capacitor with center conductor.

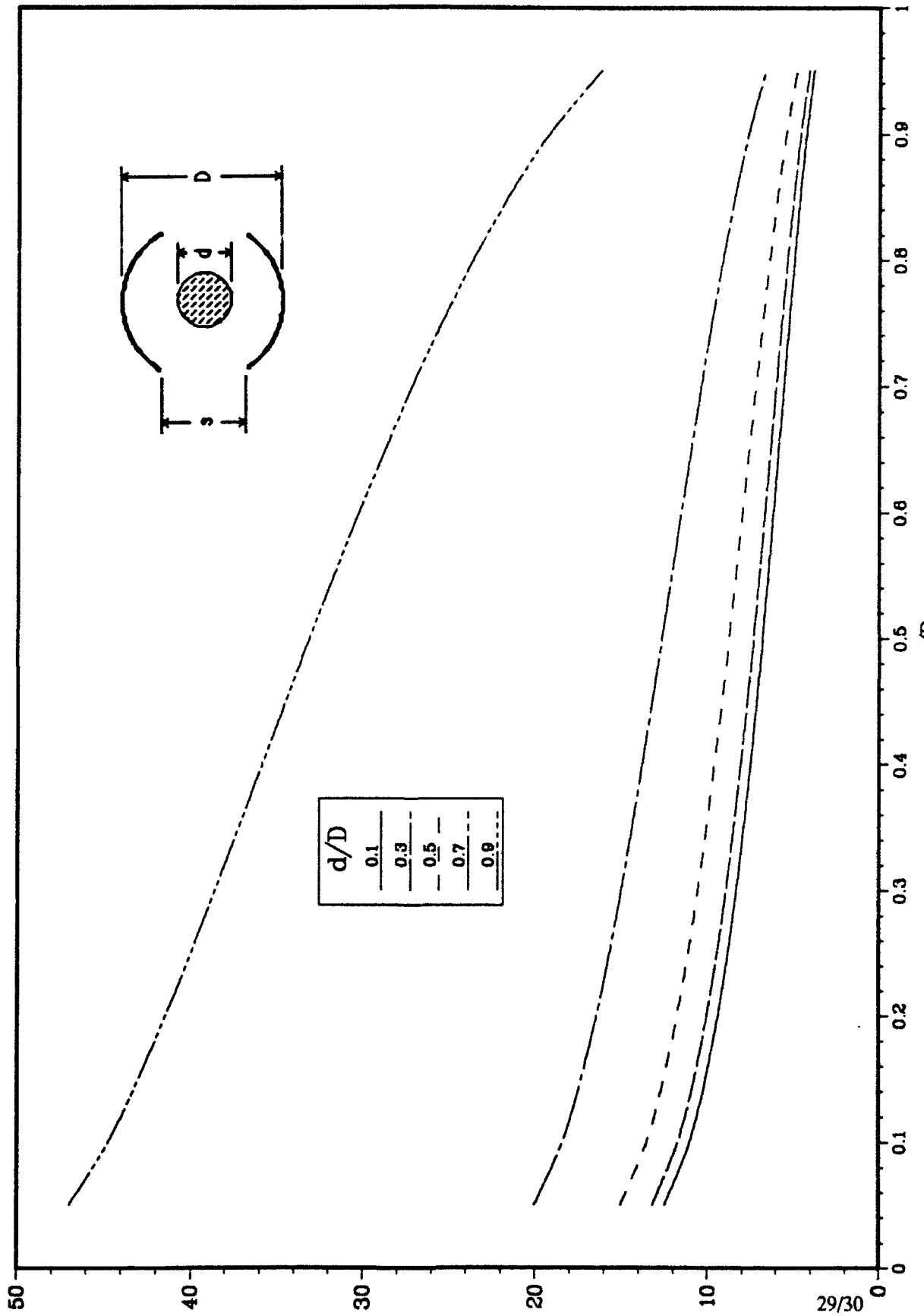

Fig. 9(b). Capacitance per unit length of a curved plate capacitor for various s/D and d/D ratios

REVERSE BLANK

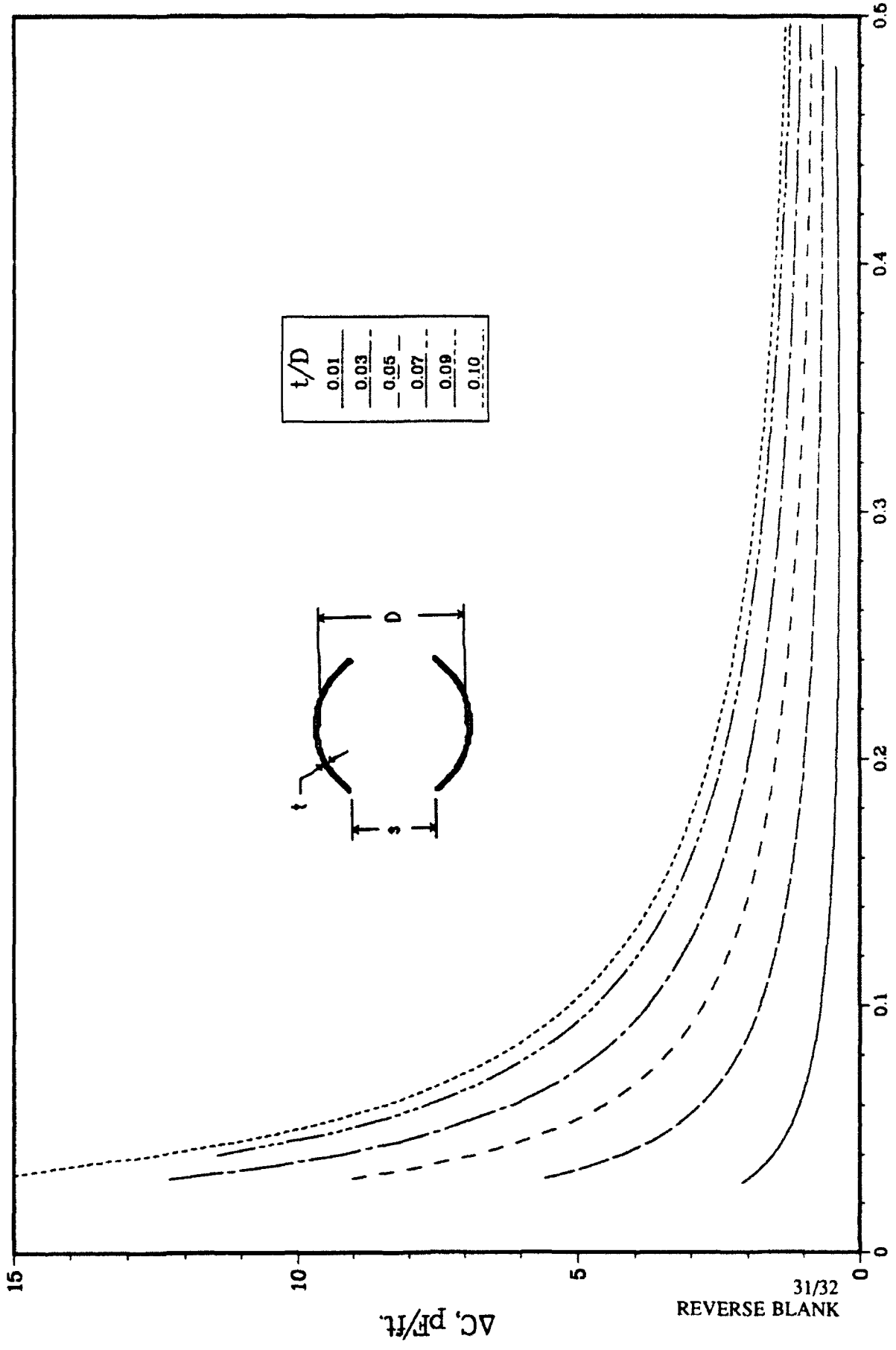

Fig. 10. Change in capacitance due to plate thickening for various s/D and t/D ratios.

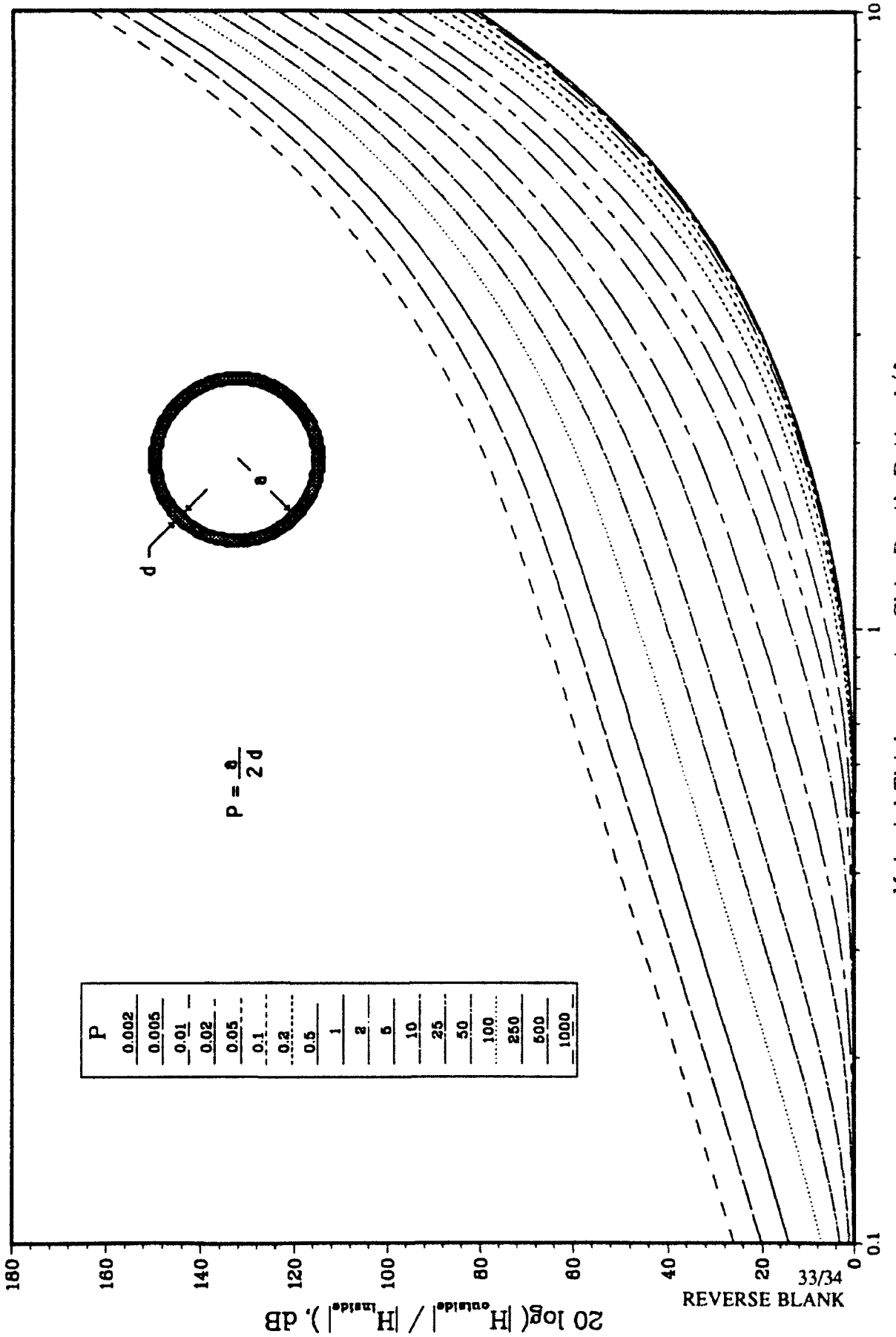

Fig. 11. Shielding effectiveness of non-magnetic ($\mu_r = 1$) cylinders.

REVERSE BLANK

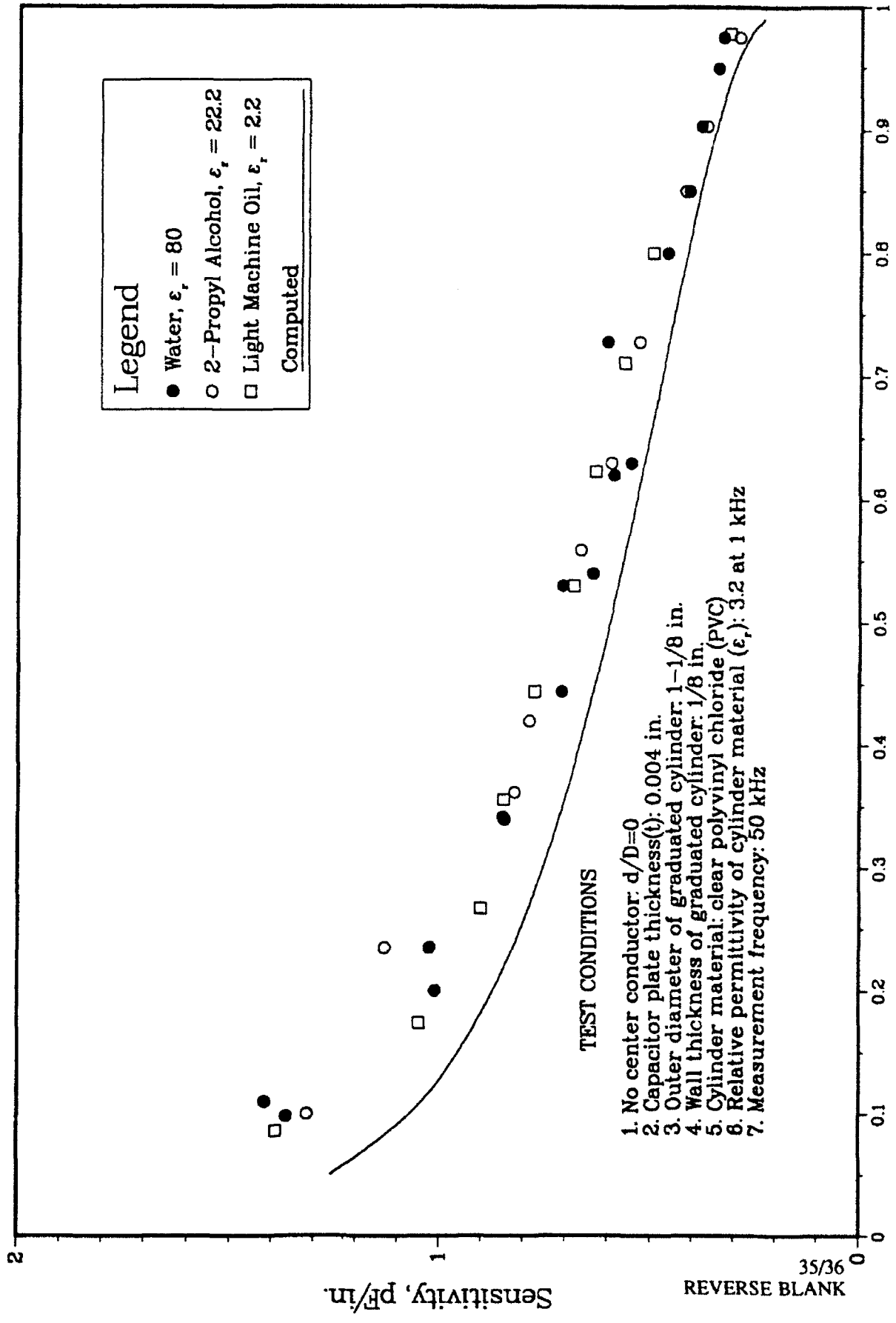

Fig. 12. Plate sensivity ($\partial C/\partial \varepsilon$) for various s/D ratios.

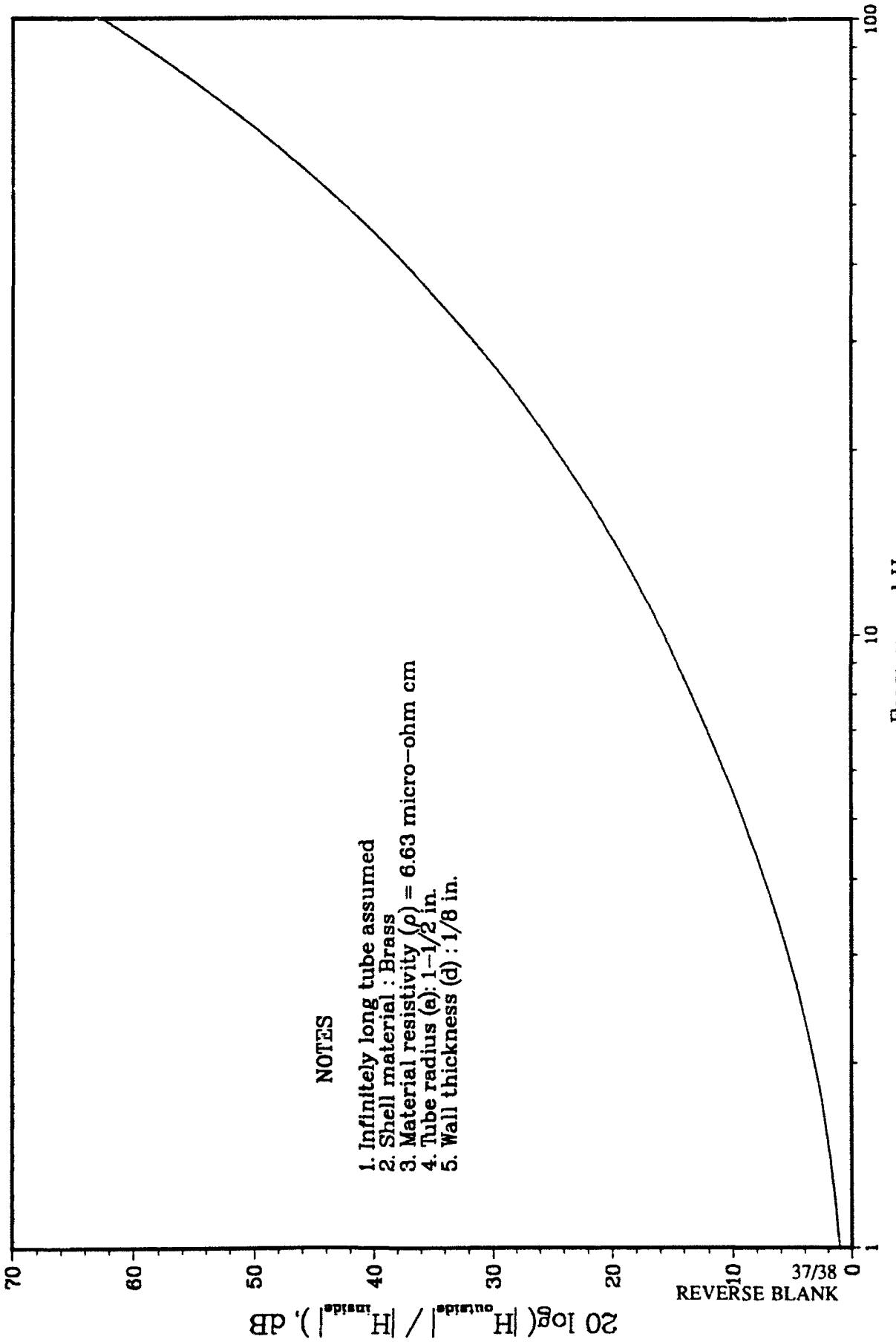

Fig. 13. Low frequency shielding effectiveness of cylinder used in the prototype

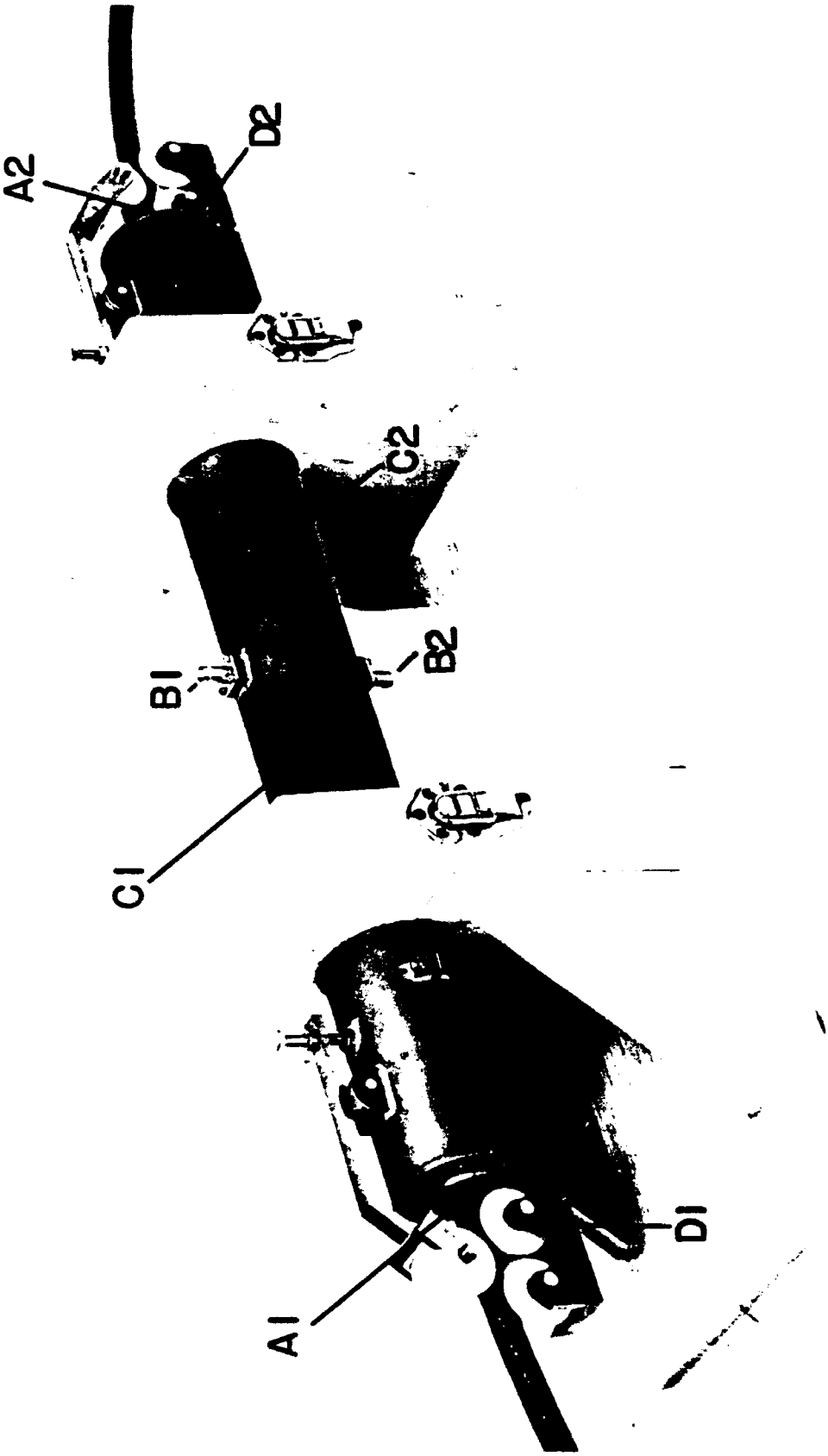

Fig. 14.

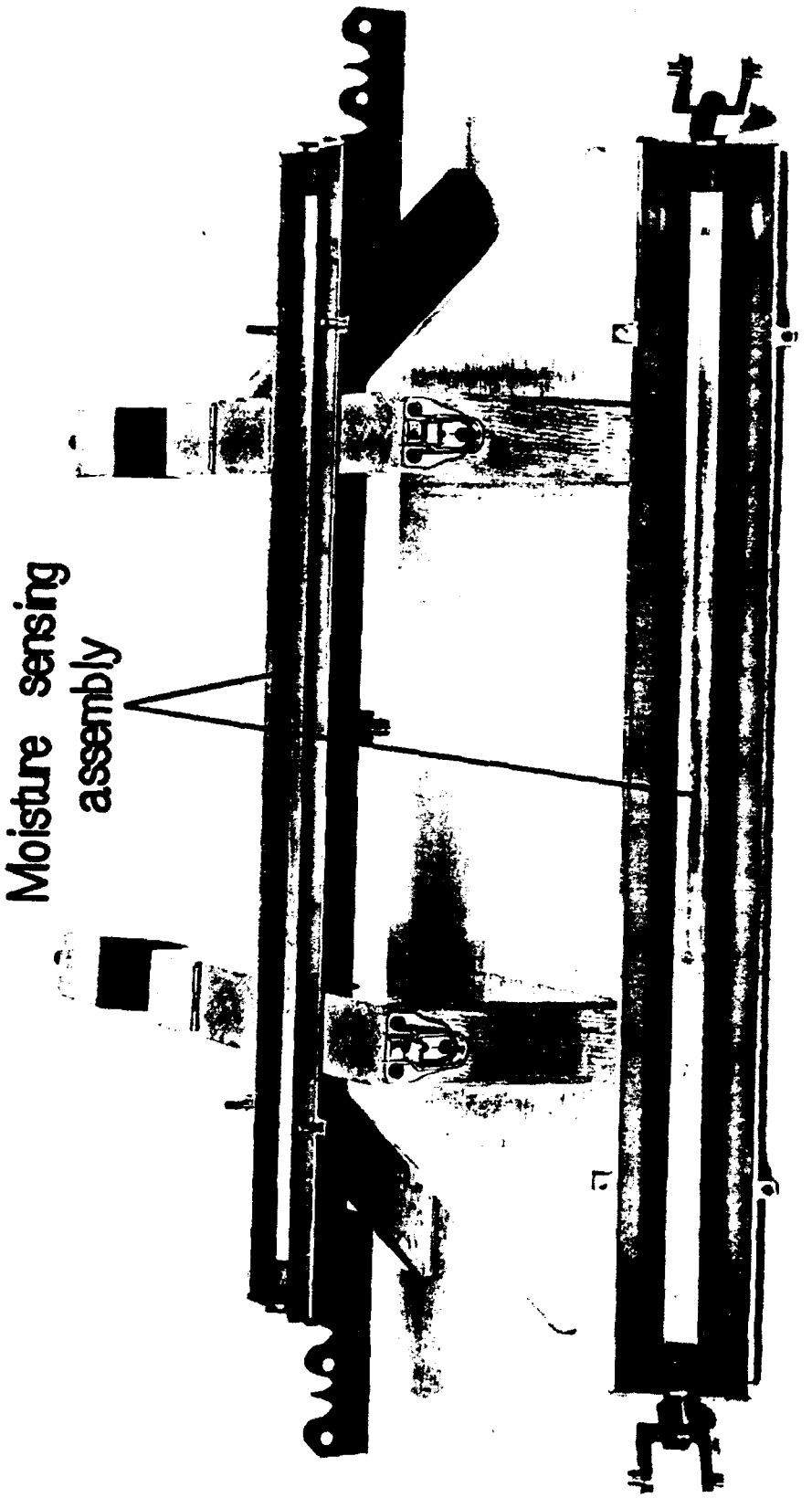

Fig. 15.

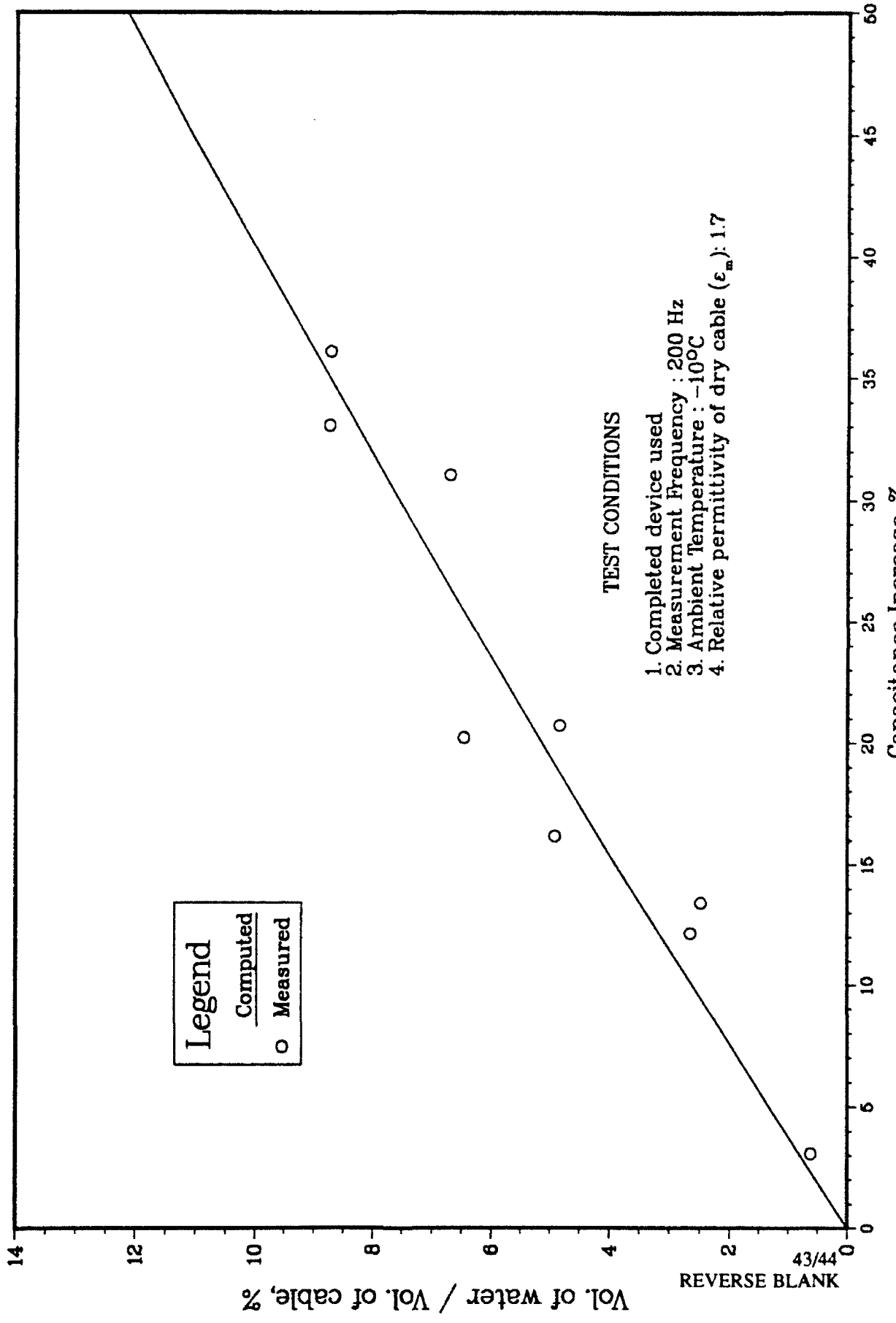

Fig. 16. Volume of water relative to cable material volume; variation with capacitance increase f. .m a (nominal) dry value.

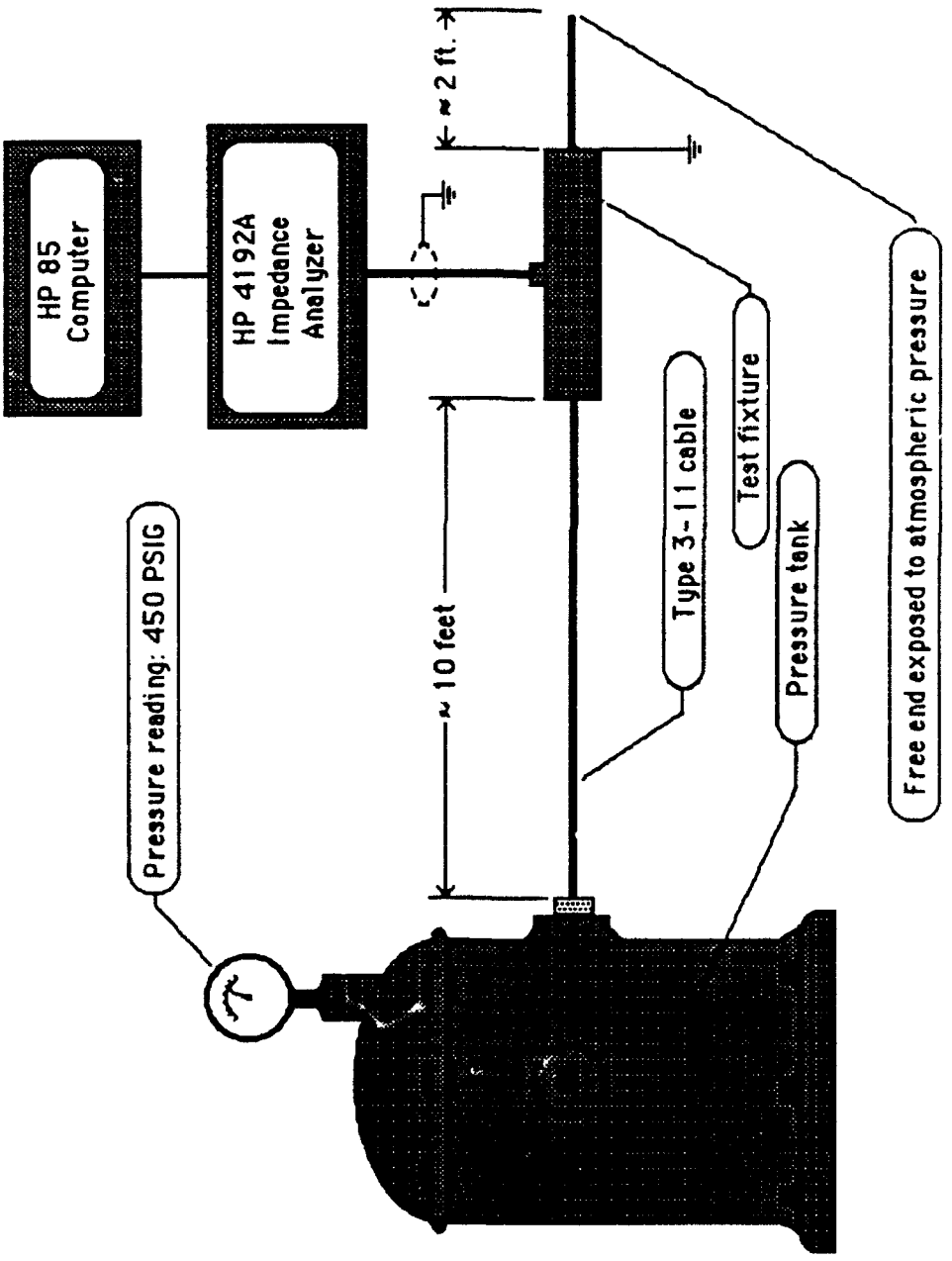

Fig. 17. Test setup to measure Φ_{max}.

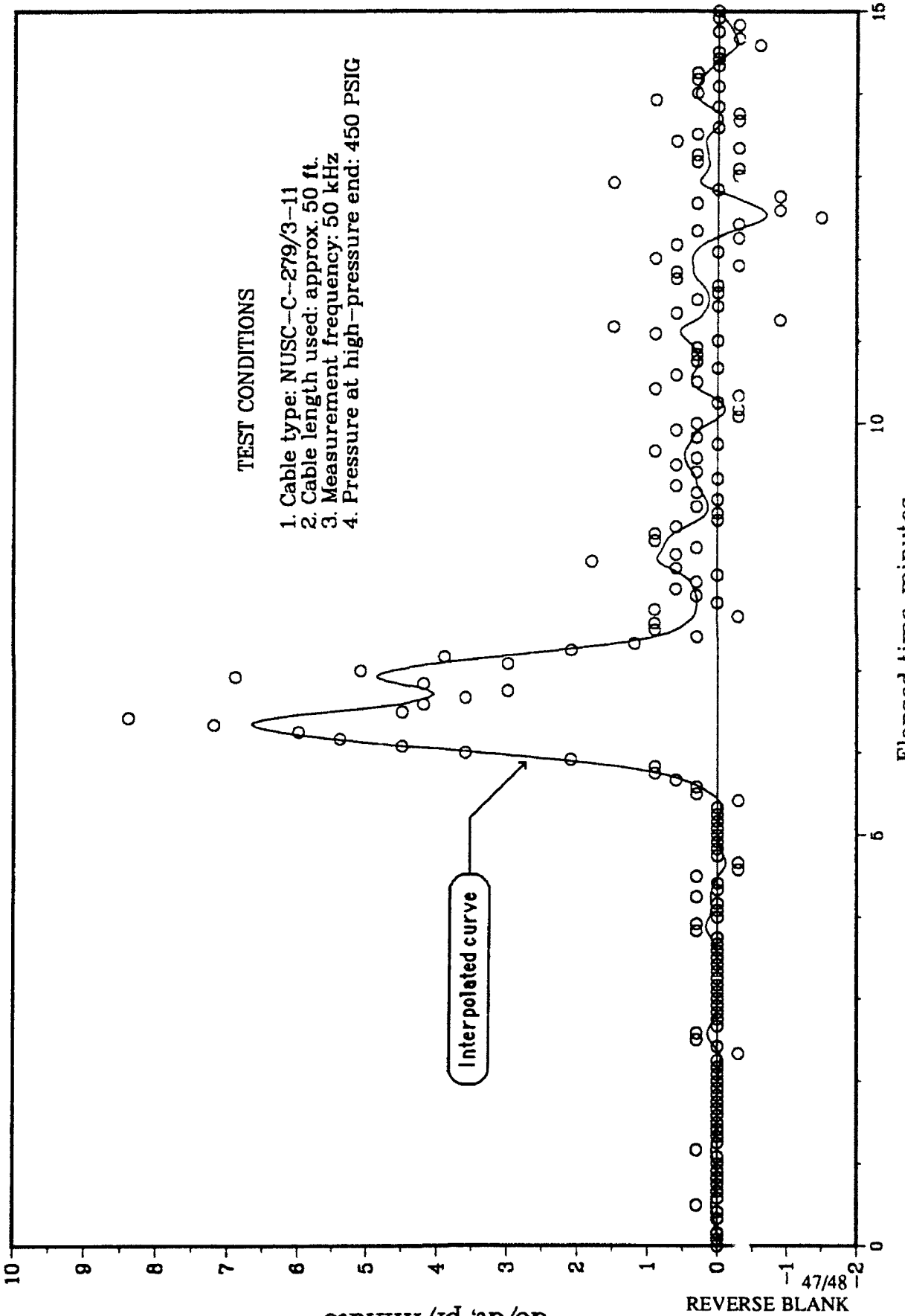

Fig. 18. Variation of Φ with time.

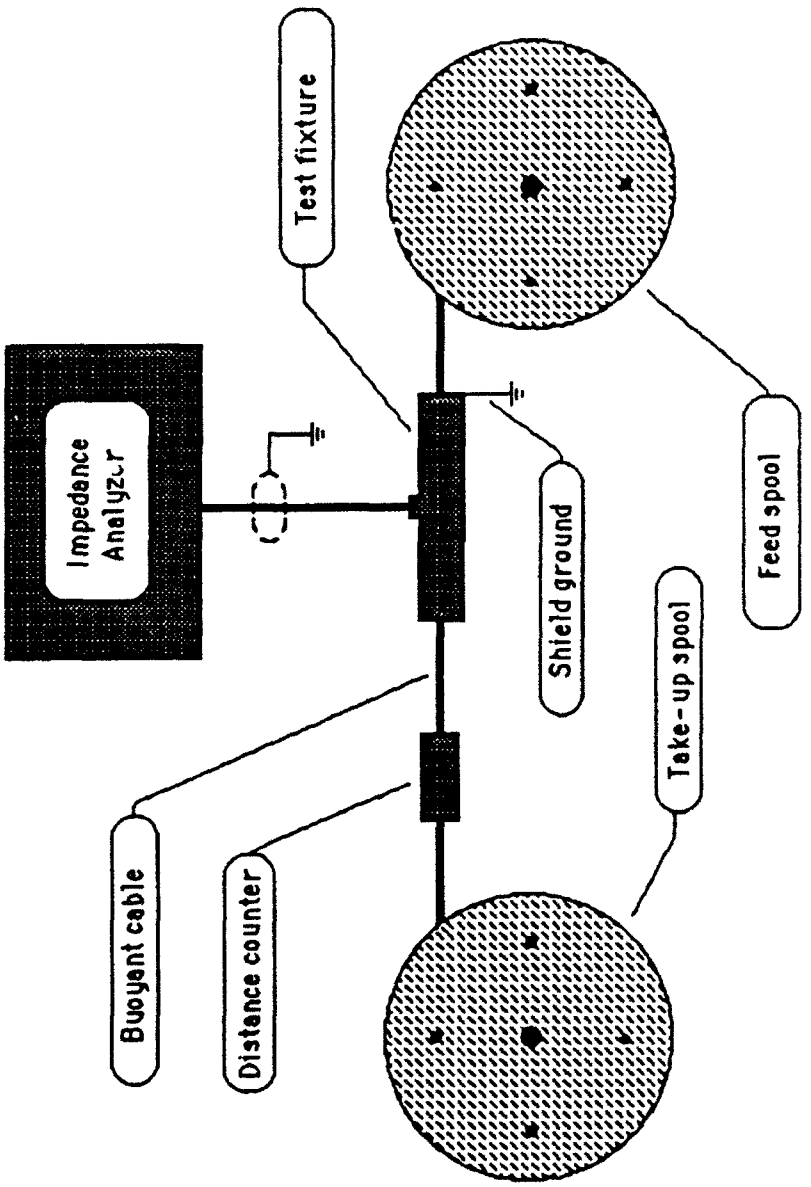

Fig. 19. Hydrostatic pressure / Capacitance test setup.

Appendix A

EXPLODED VIEW OF TEST FIXTURE

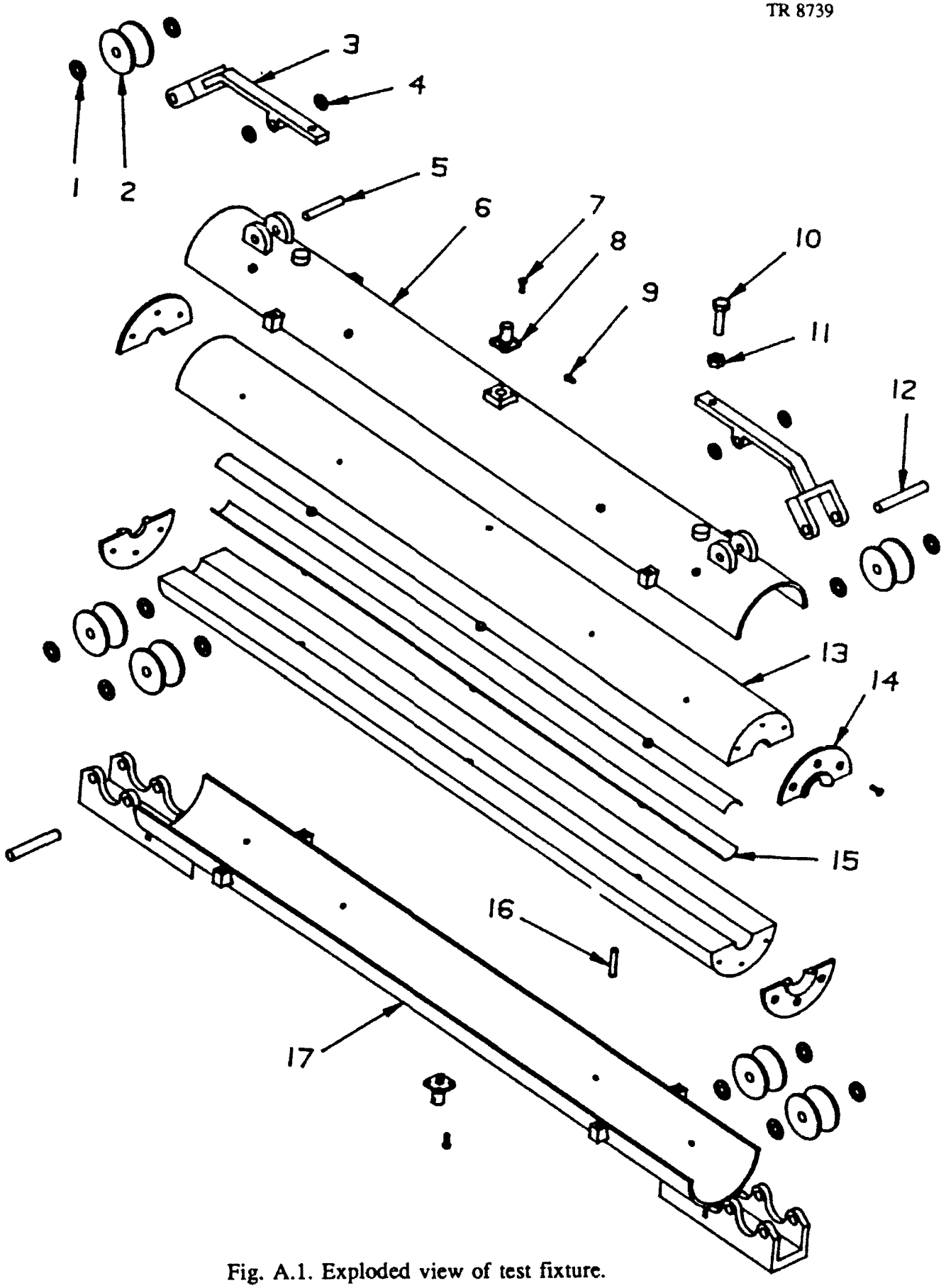

Fig. A.1. Exploded view of test fixture.

MOISTURE DETECTOR - PARTS LIST

Item Number	Quantity	Description	Overall Dimensions (inch)	Material
1	12	Washer / Spacer	5/8 O.D. X 21/64 I.D. X 0.062 Thick	Teflon
2	6	Cable Guide Roller	1.5 O.D. X 0.314 I.D. X 0.875 Thick	Teflon
3	2	Cable Tension Arm	Arm Segment : 5.937 L X 0.5 W Roller Anchor : 1.43 H X 1.5 W X 5/8 D Pivot : 0.562 H X 0.5 W X 0.5 D	Naval Brass
4	4	Washer / Spacer	0.5 O.D. X 17/64 I.D. X 0.062 Thick	Teflon
5	2	Pivot Shaft	0.25 Diam. X 1.50 L	Stainless Steel
6	1	Capacitor RF Shield / Housing (TOP)	Body : 3.00 O.D. X 2.75 I.D. X 26 L Pivot : 0.75 H X 1.0 W X 0.25 Thick Alignment Post: 0.5 H X 0.37 W X 0.37 D BNC Connector Stand : 0.75 L X 0.75 W X 0.25 D	Brass
7	8	Pan Head Machine Screw	# 4 - 40 X 3/8 L	Stainless Steel
8	2	BNC Female RF Connector	-	Nickel Plated Brass

MOISTURE DETECTOR - PARTS LIST (CON'T)

Item Number	Quantity	Description	Overall Dimensions (inch)	Material
9	28	Flat Head Machine Screw	# 4 - 40 X 3/8 L	Stainless Steel
10	2	Tension Adjust Bolt	1/4 - 20 X 1.00 L	Stainless Steel
11	2	Tension Adjust Nut	1/4 - 20 X 0.25 H	Stainless Steel
12	6	Roller Support Shaft	0.25 Diam. X 2.00 L	Stainless Steel
13	2	Capacitor Plate Support Bed	2.75 O.D. X 0.75 I.D. X 26 L	Lexan (Polycarbonate)
14	4	RF Shield End - Caps	3.00 O.D. X 0.75 I.D. X 0.125 Thick	Brass
15	2	Capacitor Plates	0.75 O.D. X 0.70 I.D. X 24 L Plate Angle of Arc : 146.8 Degrees	Brass
16	4	Housing Alignment Pins	0.1875 Diam. X 1.00 L	Stainless Steel
17	1	Capacitor RF Shield / Housing (BOTTOM)	Body : 3.00 O.D. X 2.75 I.D. X 26 L Alignment Post :0.5 H X 0.37 W X 0.37 D Cable Guide Roller Support: 5.25 L X 1.50 W X 1.56 H BNC Connector Stand : 0.75 L X 0.75 W X 0.25 D	Brass

Appendix B

ELLIPTIC INTEGRALS

1. Variable names.

Symbol	*Name*	*Domain*
k	Modulus	$0 \le k \le 1$
Ψ	Amplitude	$0 \le \Psi \le \pi/2$
ρ	Characteristic	$-\infty \le \rho \le \infty$

2. Integrals.

2.1. Elliptic integral of the first kind.

a) Incomplete

$$F(\Psi \backslash k) = \int_0^{\Psi} \frac{d\theta}{\sqrt{1 - k^2 \sin^2 \theta}} \tag{1a}$$

b) Complete

$$K(k) = F\left(\frac{\pi}{2} \backslash k\right) = \int_0^{\frac{\pi}{2}} \frac{d\theta}{\sqrt{1 - k^2 \sin^2 \theta}} \tag{1b}$$

2.2. Elliptic integral of the second kind.

a) Incomplete

$$E(\Psi \backslash k) = \int_0^{\Psi} \sqrt{1 - k^2 \sin^2 \theta}\, d\theta \tag{2a}$$

b) Complete

$$E(k) = E\left(\frac{\pi}{2} \backslash k\right) = \int_0^{\frac{\pi}{2}} \sqrt{1 - k^2 \sin^2 \theta}\, d\theta \tag{2b}$$

2.3. Elliptic integral of the third kind.

a) Incomplete

$$\Pi(\rho; \Psi \backslash k) = \int_0^{\Psi} \frac{d\theta}{(1 - \rho \sin^2 \theta)\sqrt{1 - k^2 \sin^2 \theta}} \tag{3a}$$

b) Complete

$$\Pi(\rho \backslash k) = \Pi\left(\rho; \frac{\pi}{2} \backslash k\right) = \int_0^{\frac{\pi}{2}} \frac{d\theta}{(1 - \rho \sin^2 \theta)\sqrt{1 - k^2 \sin^2 \theta}} \tag{3b}$$

Appendix C

COMPUTATION OF THE CAPACITANCE PER UNIT LENGTH OF A CURVED PLATE CAPACITOR WITH A CENTER CONDUCTOR

1. General.

An exact method and an approximate method of calculating the capacitance of a curved plate capacitor with a center conductor are given in this appendix. These methods were not used directly in the development of the test fixture, but are presented here for the sake of completeness. They show the relationship between the capacitance and the physical characteristics of the curved plate capacitor. A method of accounting for the thickness of the plates is also given.

A cross-sectional view of the capacitor is Fig. C.1. In this figure, the center conductor of diameter "d" is held at ground potential, while the upper and lower plates are set at potentials of $+V_0$ and $-V_0$, repectively. The capacitance computed from such an arrangement is called the odd-mode capacitance, and refers to the odd symmetry of the potential distribution on the plates.

1.1. Exact formula for infinitesmally-thin plates.

The exact expression for the odd-mode capacitance per unit length, found using conformal mapping techniques is given by [9]:

$$C \text{ (Farads per meter)} = 2\,\varepsilon\,\frac{K(k')}{K(k)} \tag{1a}$$

where

$$k = \frac{1}{\sqrt{1+\beta}} \quad \text{and} \quad k' = \sqrt{1-k^2} \tag{1b}$$

The parameter β is a function of the angle subtended by the plates in the gap region (φ) and the ratio D/d, and is determined from the set of simultaneous parametric equations given below:

$$\ln\left(\frac{d}{D}\right) = \frac{\left[(\alpha - 1)\,\Pi(\rho_1 \backslash \kappa_1) - (\alpha + \gamma)\,K(k_1')\right]}{\sqrt{\alpha(\beta + 1)}} \tag{2a}$$

$$\cos^{-1}\left(\frac{s}{D}\right) = \frac{\pi}{2} - \varphi = \frac{\left[(\gamma + 1)\,F(\Psi \backslash k_1) - \Pi(\rho_2\,;\,\Psi \backslash k_1)\right]}{\sqrt{\alpha(\beta + 1)}} \tag{2b}$$

and

$$\frac{\pi}{2} = \frac{\left[(\gamma - \beta)\,K(k_1) + (\beta + \alpha)\,\Pi(\rho_3 \backslash k_1)\right]}{\sqrt{\alpha(\beta + 1)}} \tag{2c}$$

where

$$k_1 = \sqrt{\frac{\beta(\alpha + 1)}{\alpha(\beta + 1)}} \quad \text{and} \quad k_1' = \sqrt{1 - k^2} \tag{3a}$$

also

$$\rho_1 = -\frac{1}{\alpha} \quad \text{and} \quad \rho_2 = -\left(\frac{\beta}{\beta + 1}\right) \tag{3b}$$

$$\rho_3 = -\left(\frac{\alpha - 1}{\beta + 1}\right) \quad \text{and} \quad \Psi = \sin^{-1}\left(\sqrt{\frac{\gamma(\beta + 1)}{\beta(\gamma + 1)}}\right) \tag{3c}$$

1.2. Approximate computation: variational formulas.

An alternate method of determining the capacitance for the configuration shown in Fig. C.1 is through the use of the Rayleigh-Ritz technique, used in the Calculus of Variations. In the present application, a mathematical expression describing the electrostatic charge distribution on the capacitor plates is chosen in a manner such that electric field energy stored in the system is a minimum. Due to the nature of this technique, an upper and lower bound for the capacitance is sought. Collin [10] has derived these bounds (converted here in terms of capacitance, Farads/meter) in the form:

a) Lower-bound capacitance:

$$C_{\text{lower bound}} = \frac{\pi}{16}\varepsilon \frac{(\pi - 2\varphi)^2}{\sum_{n=1,3,5,\ldots}^{\infty} \frac{\cos^2 n\varphi \left[1 + \zeta \frac{n^2(\pi - 2\varphi)^2}{n^2(\pi - 2\varphi)^2 - 4\pi^2}\right]^2}{n^3\left[1 + \coth\left(n \ln\frac{D}{d}\right)\right]}} \tag{4a}$$

where

$$\zeta = -\frac{\sum_{n=1,3,5,\ldots}^{\infty} \frac{\cos^2 n\varphi}{n\left[1 + \coth\left(n \ln\frac{D}{d}\right)\right]\left[n^2(\pi - 2\varphi)^2 - 4\pi^2\right]}}{\sum_{n=1,3,5,\ldots}^{\infty} \frac{[n \cos^2 n\varphi][\pi - 2\varphi]^2}{\left[1 + \coth\left(n \ln\frac{D}{d}\right)\right]\left[n^2(\pi - 2\varphi)^2 - 4\pi^2\right]^2}} \tag{4b}$$

b) Upper-bound capacitance:

$$C_{\text{upper bound}} = \frac{4}{\pi}\,\varepsilon\,\frac{\varphi^2}{\sum_{n\,=\,1,3,5,\ldots}^{\infty}\left[1+\coth\left(n\ln\frac{D}{d}\right)\right]\frac{\sin^2 n\varphi}{n^3}} \tag{4c}$$

where φ and D/d were defined in Fig. C.1. The plot in Fig. C.2 was made by computing the arithmetic average of the upper and lower bounds.

1.3. Plate thickness correction.

The problem of accounting for the finite plate thicknesses found in actual practice can be made by the addition of a correction, ΔC, to the vanishingly-thin plate capacitance computed from the expressions given earlier, with no center conductor. This assumption is made for cases where the plate thickness-to-diameter ratio (t/D) is very small ($<< 1$) and the plate shape ratio (s/D) is small (< 0.5) so that the electric field is not seriously distorted. Bochenek [11] has analyzed this problem, but the expressions, like those derived by Smolarska [12], are difficult to evaluate in their exact form. Figure C.3 illustrates the problem under consideration.

The capacitance per unit length of Fig. C.3a is found from:

$$C_1 = 2\,\varepsilon\,\frac{K(k_1')}{K(k_1)} \tag{5a}$$

where

$$k_1 = \frac{1}{\sqrt{1 + \left[\frac{E(k)}{k \sin^{-1}\left(\frac{s}{D}\right)}\right]^2}} \quad \text{and} \quad k_1' = \sqrt{1 - k_1^2} \tag{5b}$$

and k is the zero of eq (5c):

$$2 \sin^{-1}\left(\frac{s}{D}\right)\left[K(k') - E(k')\right] - \ln\left(1 + 2\frac{t}{D}\right)E(k) = 0 \tag{5c}$$

where

$$k' = \sqrt{1 - k^2} \tag{5d}$$

The capacitance per unit length of Fig. C.3b is given by Hilberg [13] as:

$$C_2 = 2\varepsilon \frac{K(k_2')}{K(k_2)} \tag{6a}$$

where

$$k_2 = \frac{s}{D} \quad \text{and} \quad k_2' = \sqrt{1 - k_2^2} \tag{6b}$$

Finally, the value of ΔC to be added to the thin-plate capacitance per unit length of a capacitor with a center conductor is found from:

$$\Delta C = C_1 - C_2 \tag{6c}$$

The plot shown in Fig. C.4 has been constructed using the expressions given above. By knowing the value of t/D and s/D, the value of ΔC is found and added to the infinitesmally-thin plate capacitance per unit length, given by Fig. C.2.

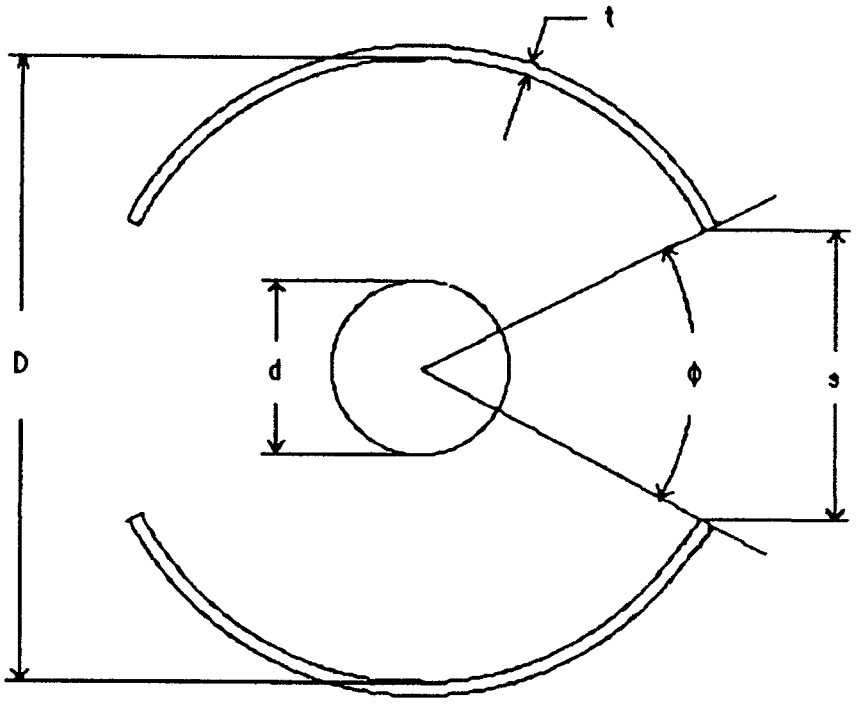

Fig. C.1. Capacitor with center conductor.

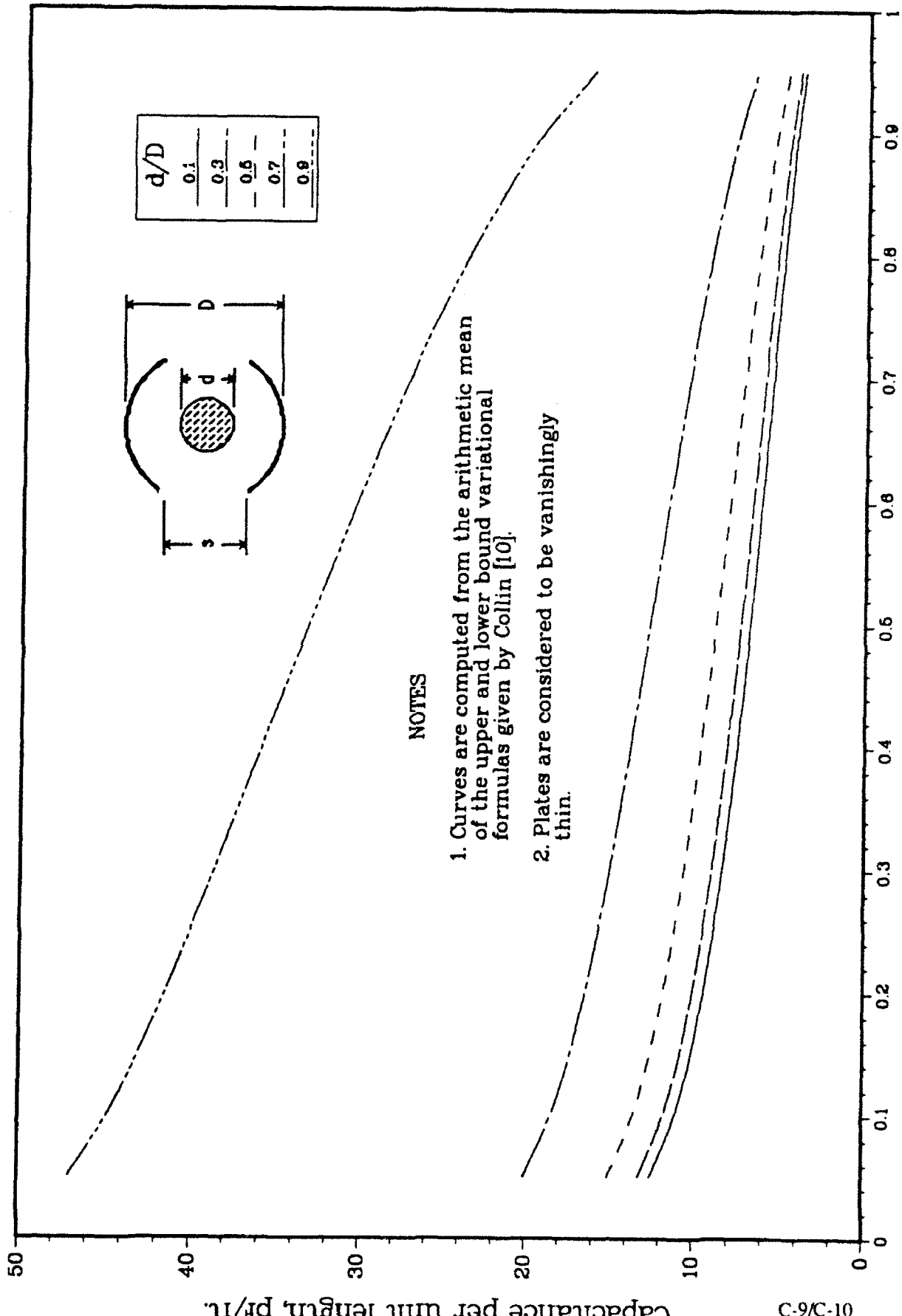

Fig. C.2. Calculated capacitance of a curved plate capacitor with a center conductor.

Small gaps are assumed: s/D < 0.5

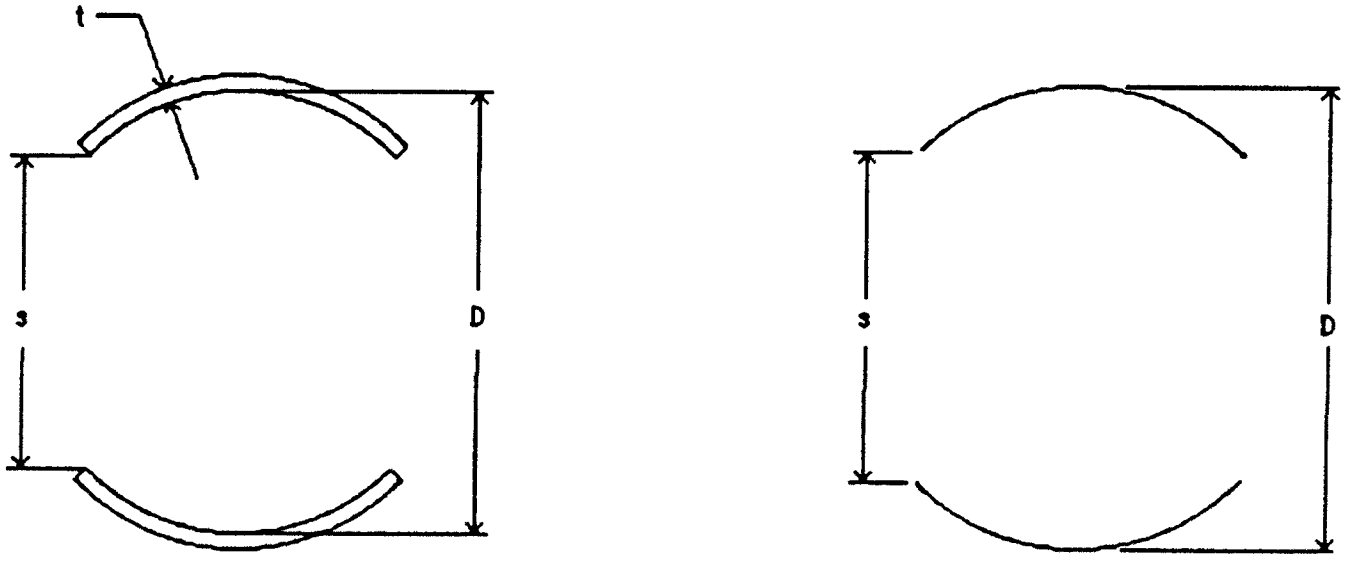

(a)

Curved plate capacitor with finite plate thickness "t" with capacitance C1

(b)

Curved plate capacitor with infinitesmally thin plates, with capacitance C2

Fig. C.3. Plate thickness correction. The correction, ΔC, is the difference of the two capacitances C1 and C2: $\Delta C = C1 - C2$.

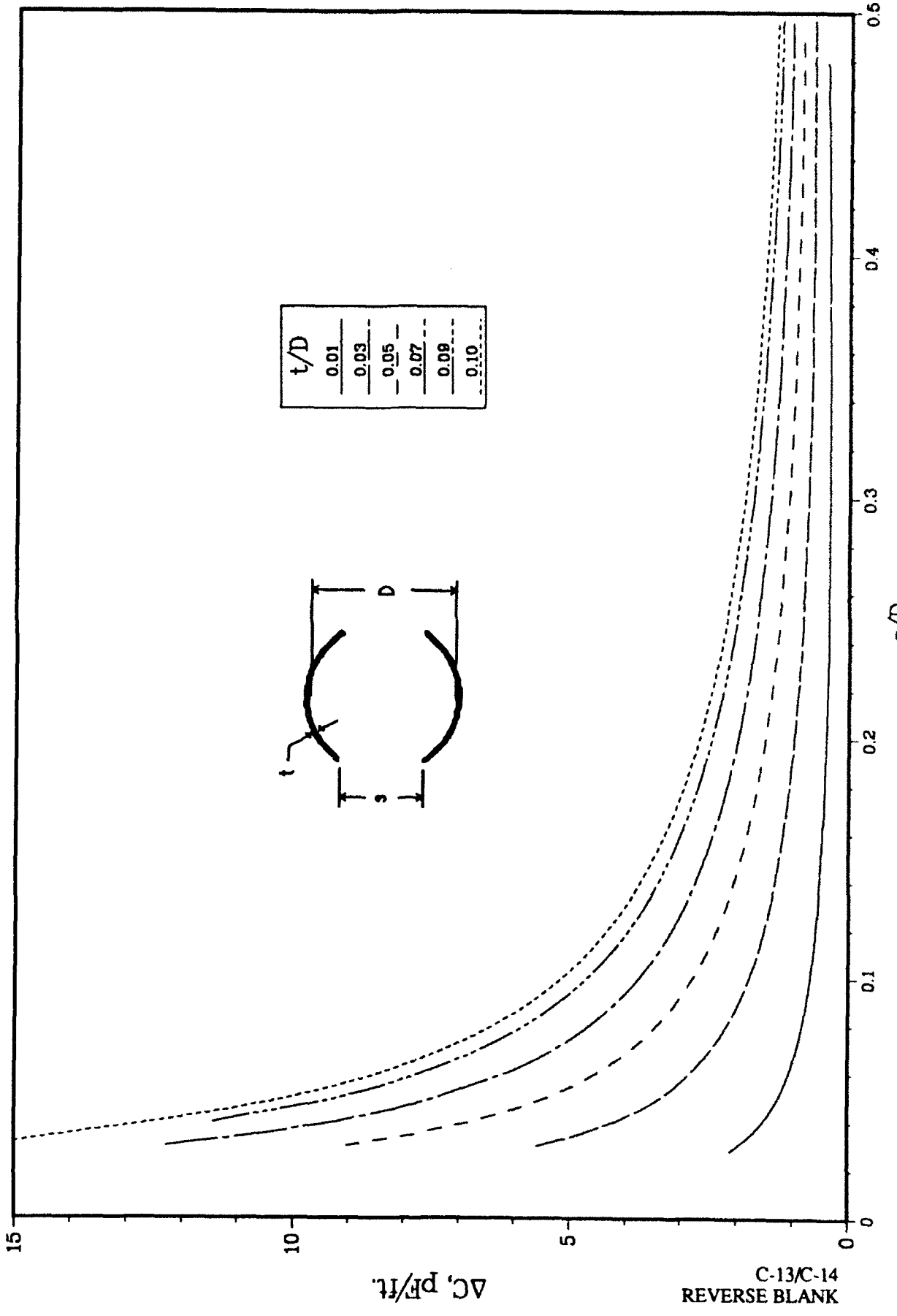

Fig. C.4. Plate thickness correction for curved plate capacitors.

Appendix D

THE DETERMINATION OF THE WATER CONTENT IN A FLOODED BUOYANT CABLE IN TERMS OF CAPACITANCE

1. Volume of water.

To arrive at an expression for the amount of water trapped in a cable in terms of capacitance, some assumptions are made to simplify the analysis. For a given length:

i) The cable is of constant volume made up of a material having uniform density and permittivity. There are voids within the cable that become filled with material

ii) The cable cross-section is uniform, i.e., no bulges or other defects are present on the cable's outer jacket

iii) The flooded cable weight is the sum of the cable's dry weight and that due to the volume of water (to be determined)

iv) The distribution of water is random within the air voids inside the cable.

Statement (iii) can be written as:

$$W_t = W_m + W_f \tag{1}$$

where

W_t = the flooded cable weight (excluding the center conductor)

W_m = the dry cable weight (excluding the center conductor)

W_f = the weight imparted by a volume of water in the cable.

Let:

ρ = density = mass / volume

g = acceleration due to gravity

V = volume

ξ = specific gravity: material density relative to water

then

$$\rho_t g V_t = \rho_m g V_m + \rho_f g V_f$$

or

$$\frac{\rho_t}{\rho_f} g V_t = \frac{\rho_m}{\rho_f} g V_m + \frac{\rho_f}{\rho_f} g V_f$$

and finally

$$\xi_t V_t = \xi_m V_m + V_f \qquad (2)$$

Since the volume of the cable remains constant, it must be composed of unequal amounts of cable material and water such that:

$$V_t = V_m + V_f \qquad (3)$$

this relation establishes bounds on the maximum possible volume that water can occupy, since the cable volume is finite.

Combining eqs. (2) and (3):

$$\xi_t\ (V_m + V_f) = \xi_m\ V_m + V_f \tag{4}$$

2. The effective permittivity of a wet cable.

The effective permittivity resulting from a mixture of substances having permittivities $\varepsilon_{1,2,3,...}$, while occupying a fraction $\vartheta_{1,2,3,...}$ of the total substance volume can be computed from [14]

$$\ln(\varepsilon^*) = \sum_{i=1}^{N} \vartheta_i \ln(\varepsilon_i) \tag{5}$$

where

ε^* = effective permittivity of the substance (the wet cable)

ϑ_i = the fraction of the total volume containing an element with a permittivity of ε_i

N = number of constituent permittivities

and

$$\sum_{i=1}^{N} \vartheta_i = 1$$

3. Quantity of water inside a cable.

The cable under consideration is composed of the insulator and a volume of water.

Let:

$$\vartheta_1 = \frac{\text{volume of cable material}}{\text{total volume}} = \frac{1 - \xi_t}{1 - \xi_m} \tag{6a}$$

$$\vartheta_2 = \frac{\text{volume of water}}{\text{total volume}} = \frac{\xi_t - \xi_m}{1 - \xi_m} \tag{6b}$$

using eq. (5):

$$\ln(\varepsilon^*) = \vartheta_1 \ln(\varepsilon_1) + \vartheta_2 \ln(\varepsilon_2) \tag{6c}$$

$$= \frac{1 - \xi_t}{1 - \xi_m} \ln(\varepsilon_1) + \frac{\xi_t - \xi_m}{1 - \xi_m} \ln(\varepsilon_2) \tag{6d}$$

solving for ξ_t,

$$\xi_t = \xi_m \left[\frac{\ln\left(\frac{\varepsilon_2}{\varepsilon^*}\right)}{\ln\left(\frac{\varepsilon_2}{\varepsilon_1}\right)} \right] + \left[\frac{\ln\left(\frac{\varepsilon^*}{\varepsilon_1}\right)}{\ln\left(\frac{\varepsilon_2}{\varepsilon_1}\right)} \right] \tag{6e}$$

(here, ξ_m is the specific gravity of the cable material ≈ 0.72).

Eq. (6e) can be rewritten in terms of capacitance. Let:

$$\varepsilon_1 = \frac{C_m}{C_{air}} \ , \ \varepsilon^* = \frac{C_t}{C_{air}}$$

where

C_{air} = the capacitance of the curved plate capacitor with a center conductor and an air dielectric

C_m = the dry cable capacitance

C_t = the wet cable capacitance

and ε_2 is the relative permittivity of water ($\approx$ 80 at 20° C).

Substitution of the capacitance ratios given above into eq. (6e), along with some algebraic manipulation, yields an expression for the total specific gravity of the flooded cable material, as:

$$\xi_t = \xi_m + \kappa\left(1 - \xi_m\right) \ln\left(\frac{C_t}{C_m}\right) \tag{7}$$

where

$$\kappa = \frac{1}{\ln\left(\frac{\varepsilon_2}{\varepsilon_1}\right)} \approx 0.26, \text{ using } \varepsilon_1 \approx 1.7.$$

The amount of water in the cable can be found using eq. (7):

$$\frac{\text{volume of water}}{\text{volume of cable}} = \frac{V_f}{V_m} = \frac{\xi_t - \xi_m}{1 - \xi_t} = \frac{\kappa \ln\left(\frac{C_t}{C_m}\right)}{1 - \kappa \ln\left(\frac{C_t}{C_m}\right)} \tag{8}$$

In eq. (8), V_m can be expressed as the difference between the total volume of the cable, V_c, and the volume of the center conductor, V_a:

$$V_m = V_c - V_a \tag{9}$$

The cable volume (V_c) can be computed from:

$$V_c = L\left(\frac{W_c}{\xi_c \rho_f g}\right) \tag{10a}$$

where W_c = the weight per unit length of the cable ≈ 0.1 lb / ft
ξ_c = the specific gravity of the cable ≈ 0.74
ρ_f = the mass density of fresh water ≈ 1.94 slug / ft ^{3} at 20° C
g = the acceleration due to gravity ≈ 32.2 ft / sec ^{2}
L = the capacitor plate length = 2 ft.

The cable volume computed from eq. (10a) is useful because it accounts for air voids in the cable. The volume of the center conductor, V_a, is simply

$$V_a = \pi a^2 L \tag{10b}$$

where a is the radius of the conductor (≈ 0.092 inch). The material volume, V_m, is then

$$V_m = L\left[\left(\frac{W_c}{\xi_c \rho_f g}\right) - \pi a^2\right] . \tag{10c}$$

Substitution of eq. (10c) into eq. (8) gives the total volume of water in the cable as:

$$V_f \approx L\left[\left(\frac{W_c}{\xi_c \rho_f g}\right) - \pi a^2\right]\left[\frac{\kappa \ln\left(\frac{C_t}{C_m}\right)}{1 - \kappa \ln\left(\frac{C_t}{C_m}\right)}\right] \tag{11}$$

where κ is defined in eq. (7). The expression given as eq. (7) in the main text gives V_f in *per unit length* terms, by dropping the plate length L in eq. (11).

4. Upper limit determination.

An upper limit for eq. (8) can be determined by assigning an extreme case when $V_f = V_m$ in eq. (4) (This condition is hypothetical. Experiments carried out on type 3-11 cables have indicated that saturation occurs when $V_f \approx 0.25\ V_m$, thus preventing further increases in capacitance from the nominal dry value). When this condition is set, eq. (4) has acquires the form

$$\xi_t = \frac{1 + \xi_m}{2} \quad . \tag{12}$$

Inserting eq. (12) into the expression for the specific gravity, eq. (7), and solving for the capacitance ratio, yields

$$\left(\frac{C_t}{C_m}\right) = \sqrt{\frac{\varepsilon_f}{\varepsilon_m}} \quad . \tag{13}$$

Appendix E

SENSITIVITY

1. General.

There are generally three ways to characterize a device's sensitivity [15] :

Tangent. For a given input variable x, an output deflection y, the sensitivity of the device, holding all other system variables constant is

$$S_t = \left(\frac{\partial y}{\partial x}\right)_{\text{other system variables remain constant}} \tag{1}$$

Chord. This measure, as the tangent, utilizes a y versus x profile to define S. It, however, differs from the tangential case since it uses the end points of the profile, through which a straight line is drawn. The slope of this line, or chord, is the sensitivity:

$$S_c = \frac{y_2 - y_0}{x_2 - x_0} \tag{2}$$

Secant. This means of defining output deflection to input change, is used to specify a nominal sensitivity for a given range. In mathematical terms, it is defined in a manner identical to that of the chord, except that the end points are confined to a smaller region of interest within the profile:

$$S_s = \frac{y_2 - y_1}{x_2 - x_1} \tag{3}$$

Because of this definition, several secant sensitivities are used to specify an instrument's responsiveness. Fig. E.1 shows a graphical definition of the terms discussed above.

From the foregoing discussion, it is seen that there are three distinct ways in which to specify instrument sensitivity. Since the capacitor under consideration varies non-linearly with the plate gap-to-diameter ratio (s/D), the tangential sensitivity (S_t) was chosen as the measure of effectiveness for the device. The plate tangential sensitivity, borrowing the earlier definition, becomes:

$$S_t = \frac{\partial C}{\partial \varepsilon} = \psi \frac{\partial C}{\partial x} \tag{4}$$

The independent variable x is chosen to be the length of the capacitor containing a dielectric. An increase in the length of the dielectric will cause a capacitance rise (deflection) that will depend on the ratio, s/D. The constant of proportionality, ψ, relates $\partial C/\partial x$ to $\partial C/\partial \varepsilon$ and is discussed in § 2.1.

2. Sensitivity experiment.

In order to experimentally determine the tangential sensitivity, a test fixture, shown in Fig. E.2, was made. It was constructed from thin-walled plastic tubing. Along its length, notches were made at half-inch intervals for a total of one foot and thin capacitor plates (4 mils) were affixed on the tube's outer surface.

With the plates cut to a given width (fixing the value of s/D), the sensitivity was determined by filling the cylinder with a fluid having a known relative permittivity at the interval markings along the side of the tube. Figures E.3, E.4 and E.5 show that the capacitance varies linearly with fluid level for different values of s/D, enabling the sensitivity to be determined. Figure E.6 is a plot of the slopes computed for each line (for the three fluids used), as a function of s/D, where the slopes are seen to vary inversely with the plate gap separation. Figure E.7 is a plot of $\partial C/\partial \varepsilon$ computed from Figs. E.3 through E.6.

2.1. Derivation of $\partial C/\partial \varepsilon$.

a) Theoretical result.

The total capacitance of the configuration shown in Fig. E.8 is:

$$C_{total} = \left[\varepsilon_{r,\,eff}^{(1)}(l - h) + \varepsilon_{r,\,eff}^{(2)}(h)\right] C_o \tag{5}$$

where

C_o = capacitance in air (no dielectric)

$\varepsilon_{r,\,eff}^{(1)}$ = effective relative permittivity of empty tube

$\varepsilon_{r,\,eff}^{(2)}$ = effective relative permittivity of tube filled with fluid

h = the fluid height in the tube

l = the tube length

Let:

$$\frac{\partial C}{\partial \varepsilon} = \frac{\partial C}{\partial h} \cdot \frac{\partial h}{\partial \varepsilon} \tag{6}$$

and

$$\frac{\partial C}{\partial h} = \left[\varepsilon_{r,\,eff}^{(2)} - \varepsilon_{r,\,eff}^{(1)}\right] C_o \tag{7a}$$

$$\frac{\partial \varepsilon}{\partial h} = \left[\varepsilon_{r,\,eff}^{(2)} - \varepsilon_{r,\,eff}^{(1)}\right] \tag{7b}$$

multiplication of eqs. (7a) and (7b) yields the tangential sensitivity as:

$$\frac{\partial C}{\partial \varepsilon} = \left[\varepsilon_{r,\,eff}^{(2)} - \varepsilon_{r,\,eff}^{(1)}\right] C_o \times \frac{1}{\left[\varepsilon_{r,\,eff}^{(2)} - \varepsilon_{r,\,eff}^{(1)}\right]} = C_o \,. \tag{8}$$

b) Comparison of theoretical result with measurement.

In the present measurements, we have $\partial C/\partial h$. To obtain $\partial C/\partial \varepsilon$, the expression,

$$\frac{\partial C}{\partial \varepsilon} = \psi \frac{\partial C}{\partial h}$$

is used. In the expression, ψ is the reciprocal of the expression for $\partial \varepsilon / \partial h$ given in part (a). We must, therefore, find an expression for ψ in terms readily measured parameters. The derivation for ψ is as follows:

1. We note the following:

$$\varepsilon_{r,\,eff}^{(2)} = \frac{C_{full\ tube}}{C_o} \tag{9a}$$

$$\varepsilon_{r,\,eff}^{(1)} = \frac{C_{empty\ tube}}{C_o} \tag{9b}$$

2. Casey [16] has derived an expression that gives the effective dielectric constant of a curved plate capacitor (no center conductor) with an interior filled with a dielectric, and an air exterior as:

$$\varepsilon_{r,\,eff} = \frac{1 + \varepsilon_r}{2} \tag{10}$$

where ε_r is the relative permittivity of the interior medium.

3. The determination of ε_r is complicated by the fact that it is composed of a tube filled with a fluid. King [17] gives an approximate expression for the case where the surface of a dielectric mixture is perpendicular to the direction of the electric field (present case), as:

$$\frac{1}{\varepsilon_r} = \frac{p}{\varepsilon_{r(1)}} + \frac{1 - p}{\varepsilon_{r(2)}} \tag{11}$$

where

$\varepsilon_{r(1)}$ = the relative permittivity of the plastic tube (= 3.2)

$\varepsilon_{r(2)}$ = the relative permittivity of the fluid in the tube

p = the fraction of the total volume occupied by medium 1 (the tube)

$$= \frac{V_{\text{empty tube}}}{V_{\text{total}}} = \frac{\frac{\pi}{4}\left(d_o^2 - d_i^2\right) l}{\frac{\pi}{4} d_o^2 l} = 1 - \left(\frac{d_i}{d_o}\right)^2$$

4. From the foregoing discussion, we now write:

$$\varepsilon_{r,\,\text{eff}}^{(2)} = \frac{1 + \varepsilon_{r,\,\text{full tube}}}{2} \tag{12a}$$

$$\varepsilon_{r,\,\text{eff}}^{(1)} = \frac{1 + \varepsilon_{r,\,\text{empty tube}}}{2} \tag{12b}$$

then:

$$\varepsilon_{r,\,eff}^{(2)} - \varepsilon_{r,\,eff}^{(1)} = \left\{\frac{1 + \varepsilon_{r,\,\text{empty tube}}}{2}\right\} \cdot \left\{\frac{1 + \varepsilon_{r,\,\text{full tube}}}{1 + \varepsilon_{r,\,\text{empty tube}}} - 1\right\} \qquad (12c)$$

$$= \left\{\frac{1 + \varepsilon_{r,\,\text{empty tube}}}{2}\right\} \cdot \left\{\frac{C_{\text{full tube}}}{C_{\text{empty tube}}} - 1\right\}$$

therefore

$$\frac{\partial C}{\partial \varepsilon} = \frac{\left(\frac{\partial C}{\partial h}\right)}{\left\{\frac{1 + \varepsilon_{r,\,\text{empty tube}}}{2}\right\} \cdot \left\{\left(\frac{C_{\text{full tube}}}{C_{\text{empty tube}}} - 1\right)\right\}} . \qquad (13)$$

Given :

$d_i = 1$ inch

$d_o = 1 - 1/8$ inch

$\varepsilon_{r\,(1)} \approx 3.2$

$\varepsilon_{r\,(2)} = 1$ (air)

then:

$$\varepsilon_{r,\,\text{empty tube}} \approx 1.17 \quad \text{and} \quad \varepsilon_{r,\,eff}^{(1)} = \frac{1 + \varepsilon_{r,\,\text{empty tube}}}{2} \approx 1.08.$$

The quantities $C_{\text{full tube}}$, $C_{\text{empty tube}}$ and $\partial C/\partial h$ are taken from Figs. E.3 through E.6 and are substituted in the expression(s) given earlier, resulting in the plot of Fig. E.7. The solid curve is the capacitance per unit length computed using the equations derived by Bochenek and Hilberg [2,3].

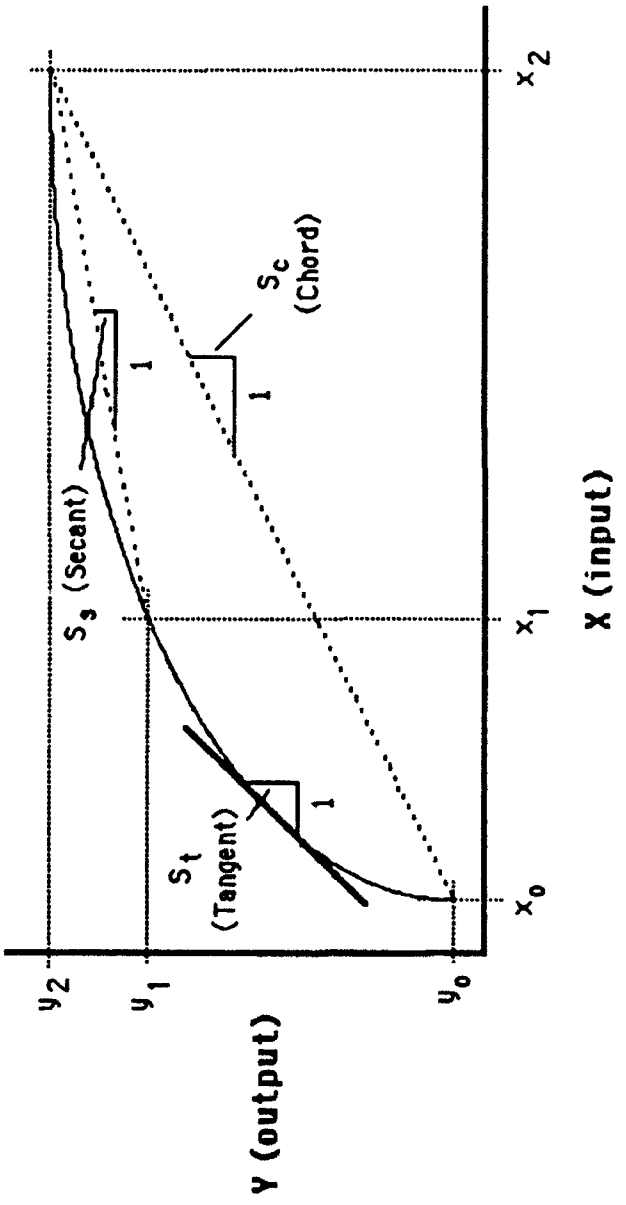

Fig. E.1. Graphical definition of sensitivity.

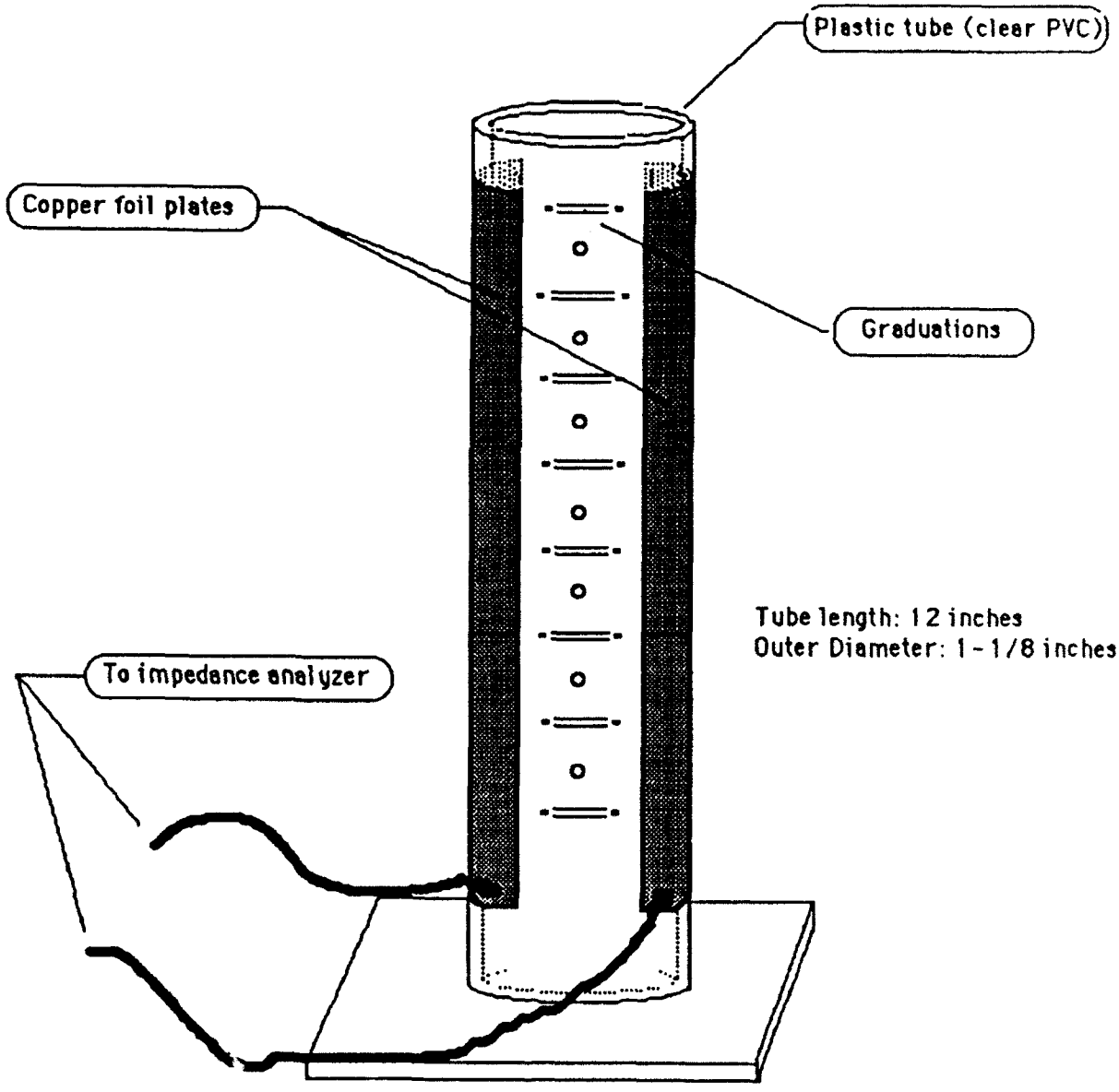

Fig. E.2. Test fixture used for sensitivity measurements.

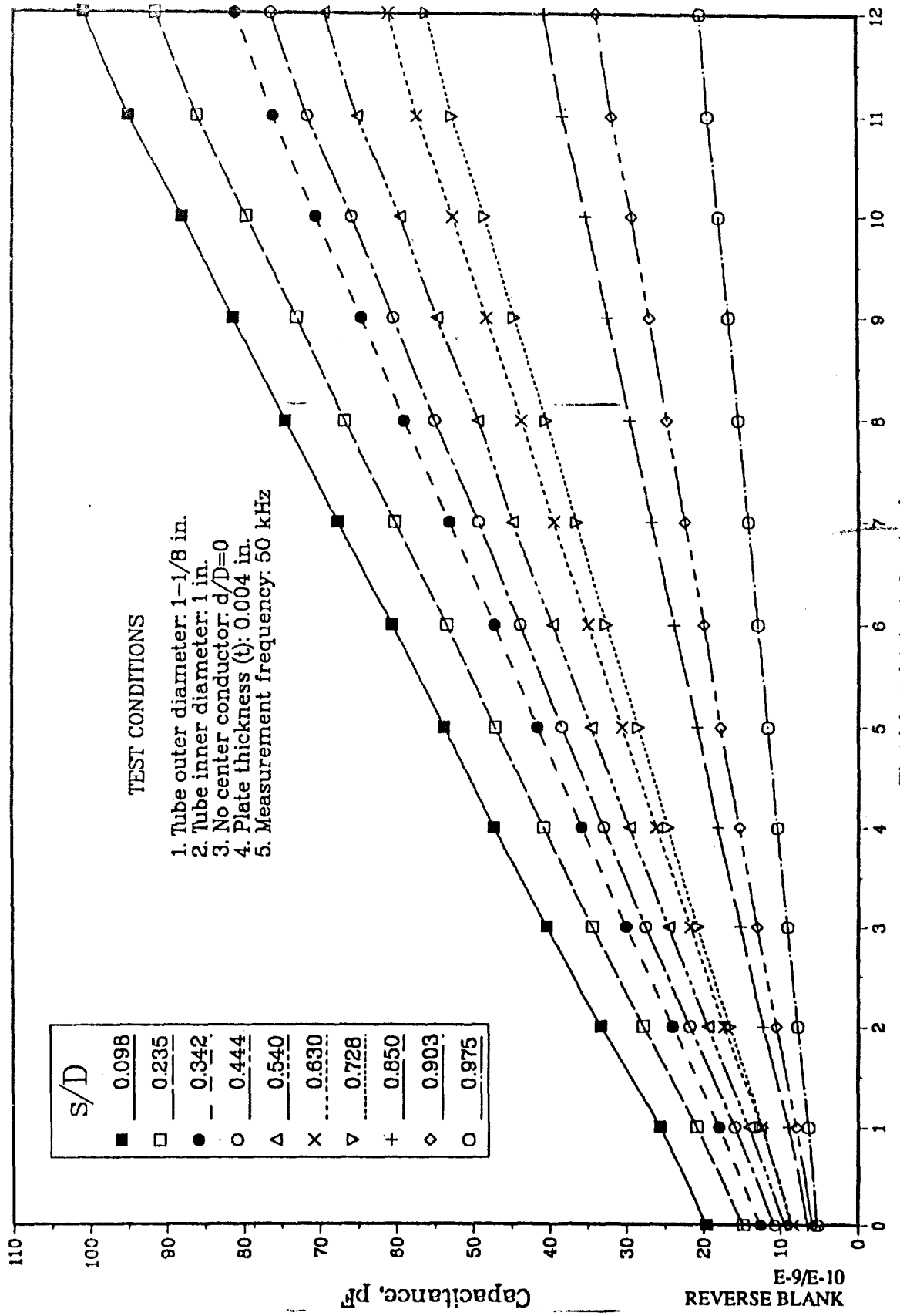

Fig. E.3. Sensitivity test; capacitance vs. fluid (water, $\varepsilon_r = 80$) level in the graduated cylinder.

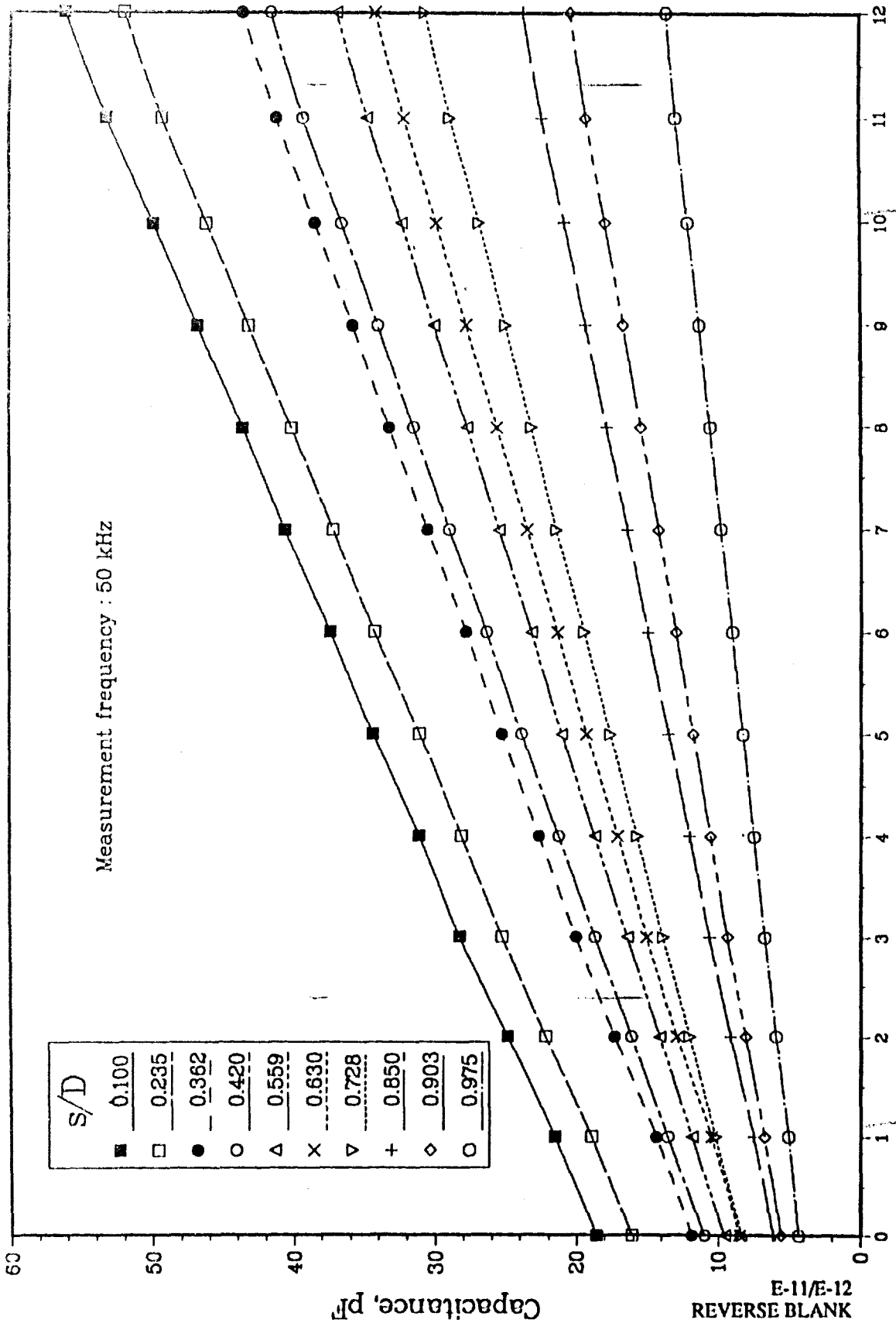

Fig. E.4. Sensitivity test; capacitance vs. fluid (2-Propyl Alchohol, $\varepsilon_r = 22.2$) level in the graduated cylinder.

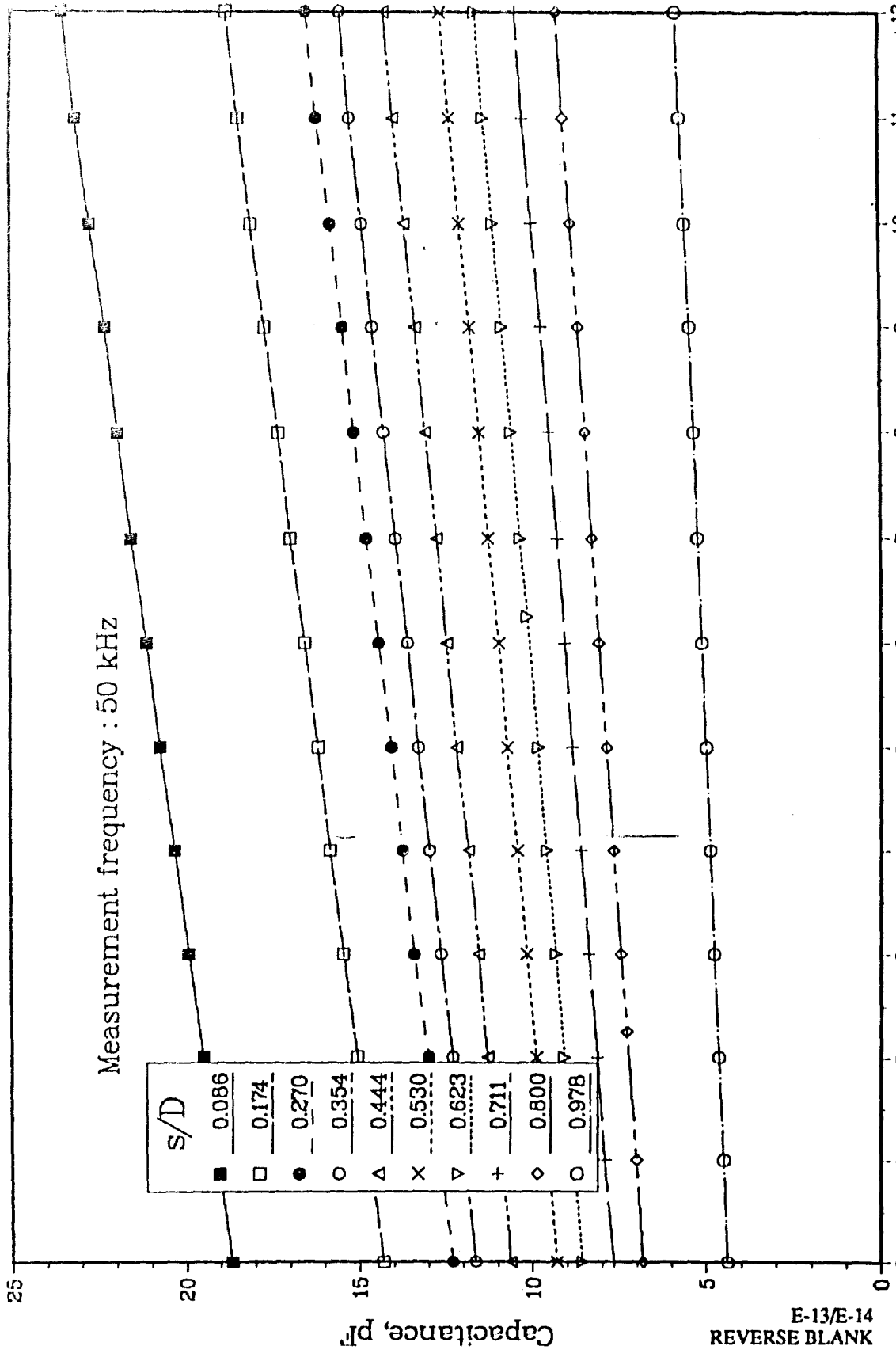

Fig. E.5. Sensitivity test; capacitance vs. fluid (Light Machine Oil, $\varepsilon_r = 2.2$) level in the graduated cylinder.

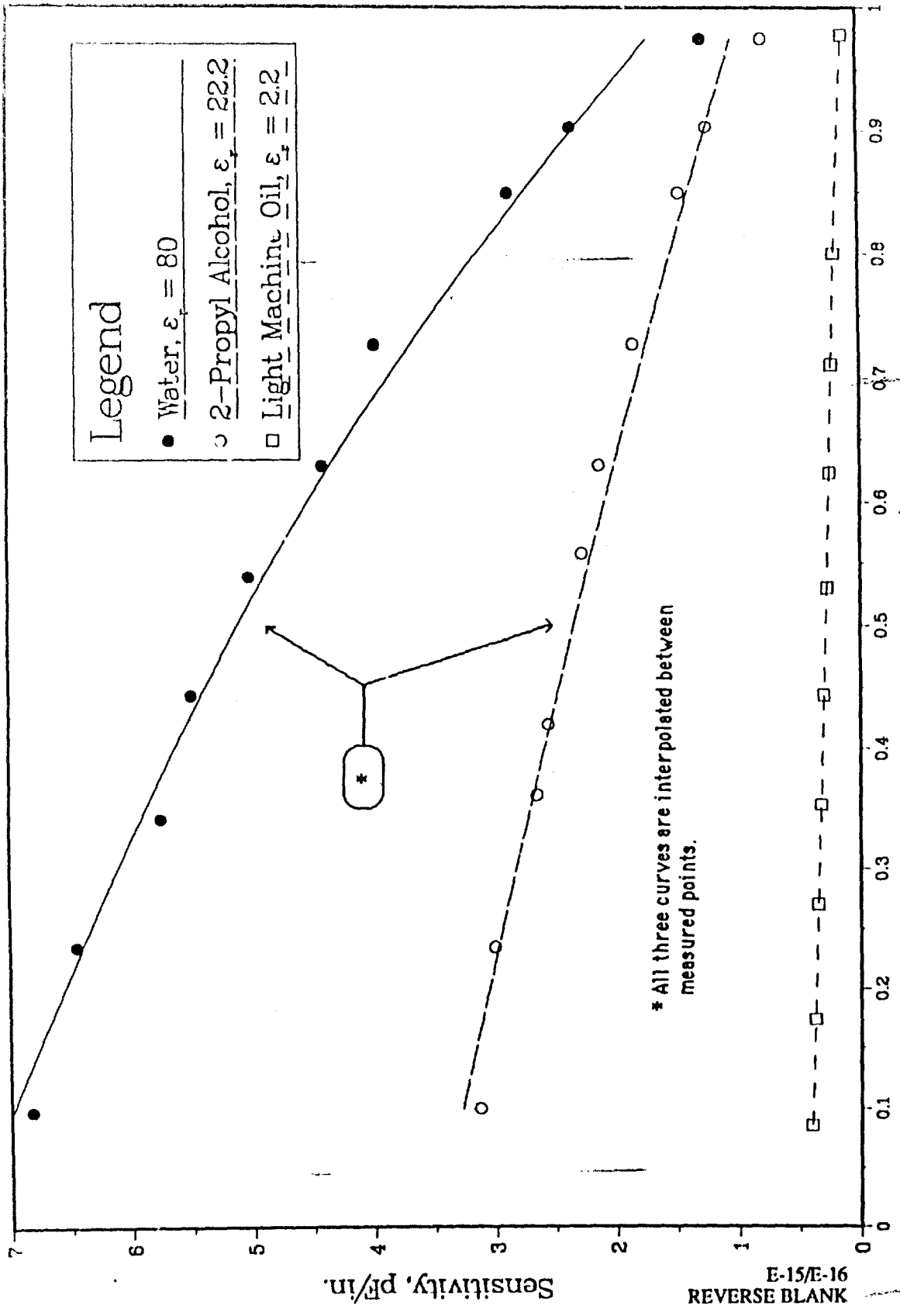

E-15/E-16
REVERSE BLANK

Fig. E.6. Variation of $\partial C/\partial h$ with s/D.

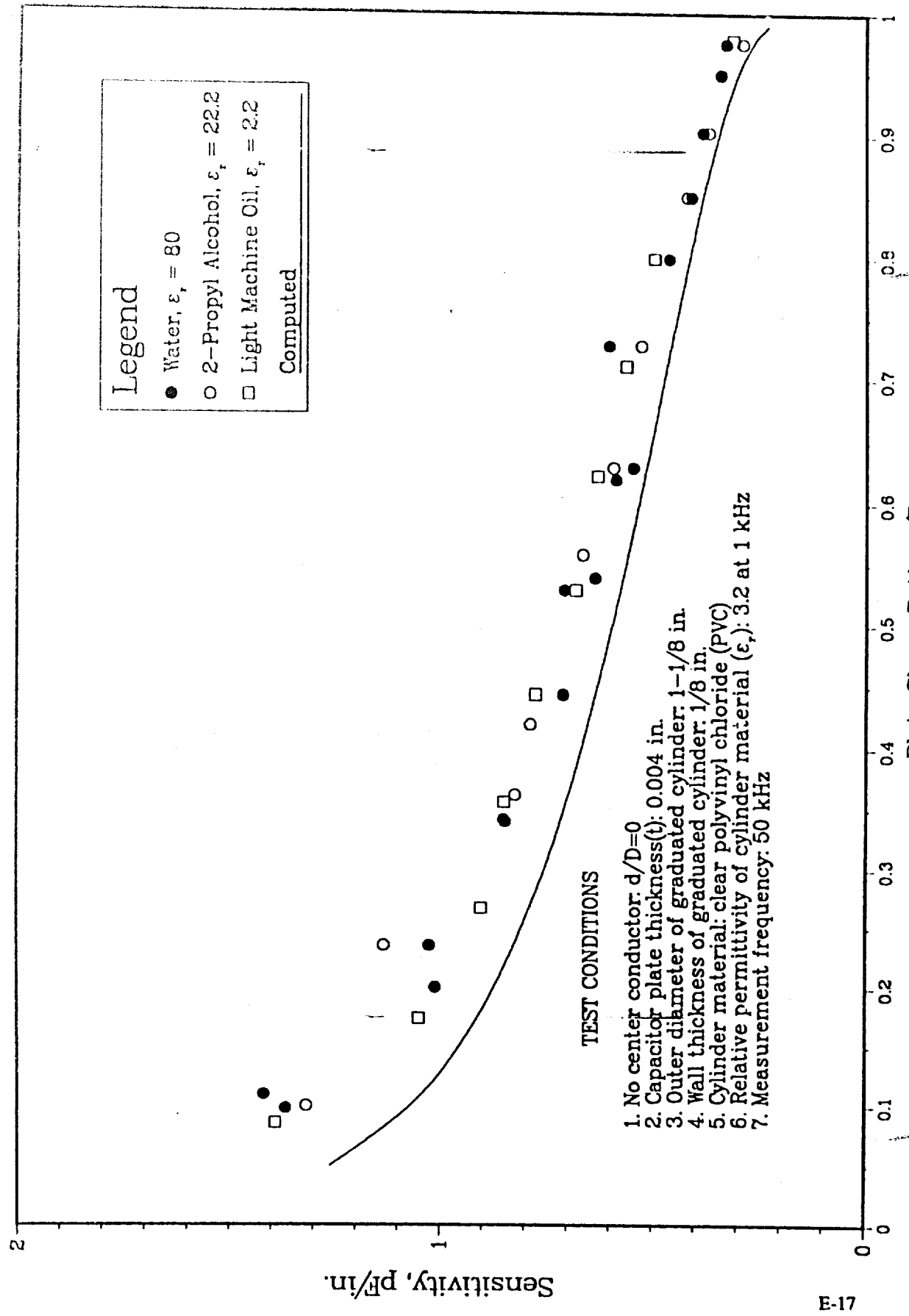

Fig. E.7. Variation of Plate Sensitivity ($\partial C/\partial \varepsilon$) with s/D.

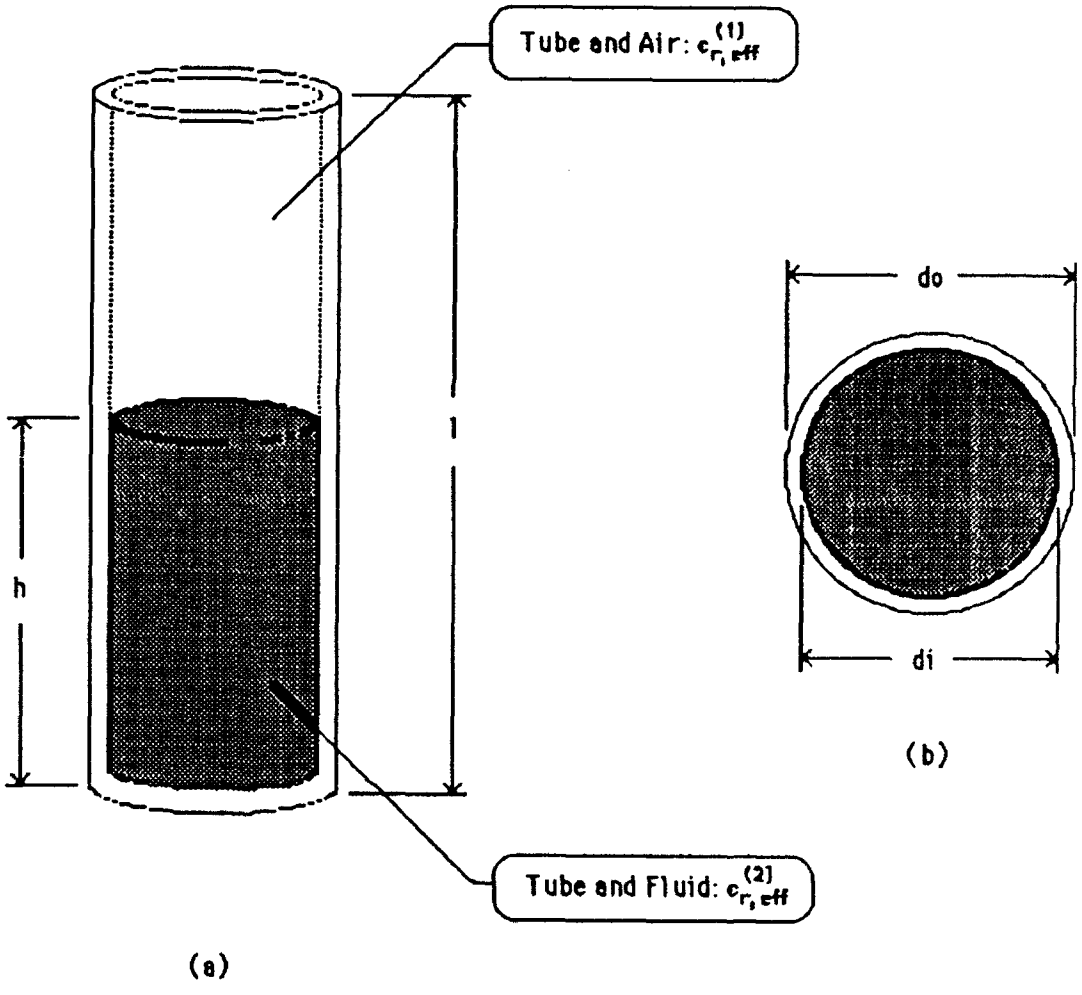

Fig. E.8. Computation of $\partial C/\partial \epsilon$. (a) Side view of tube with fluid; (b) Top view. The plates affixed to tube are not shown for clarity.

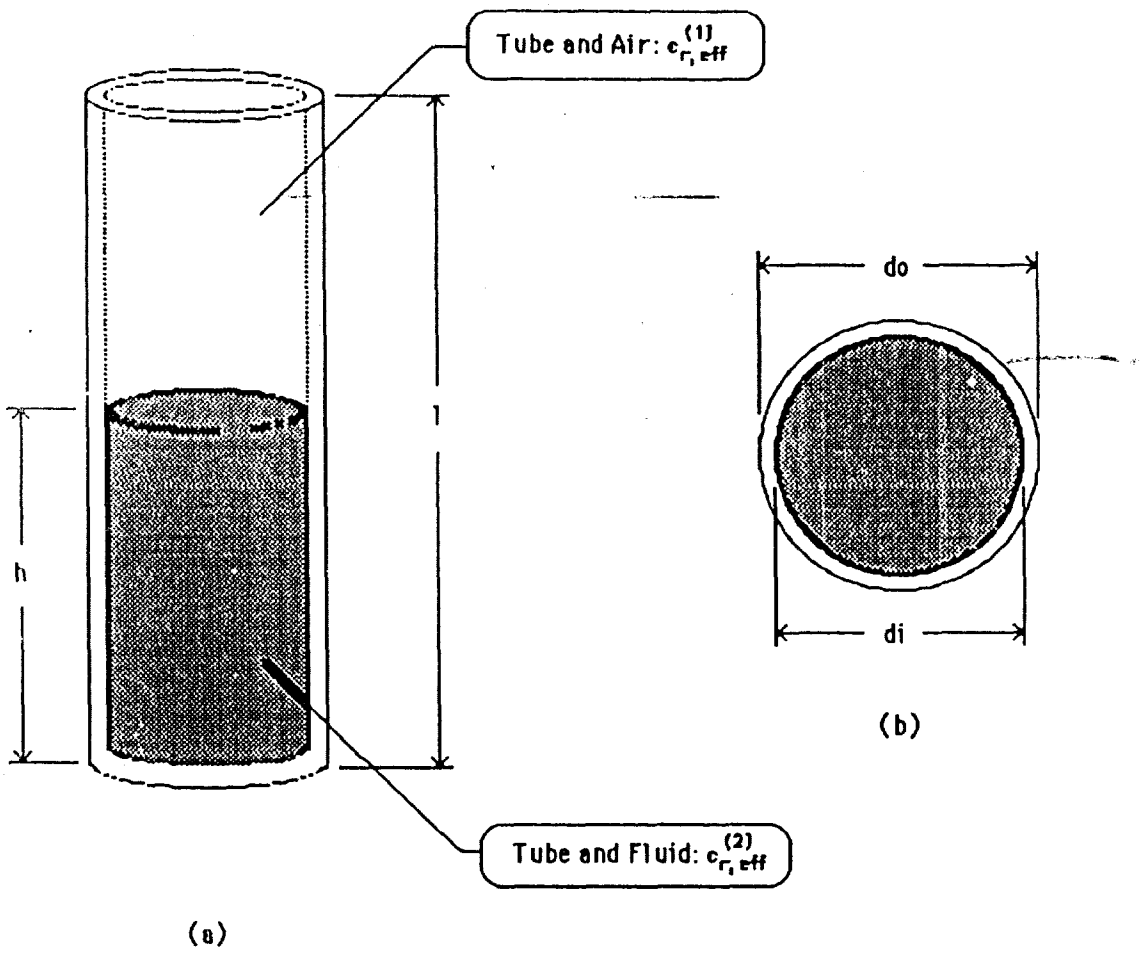

Fig. E.8. Computation of $\partial C/\partial \epsilon$. (a) Side view of tube with fluid; (b) Top view. The plates affixed to tube are not shown for clarity.

References

[1] Smolarska, J. "Characteristic Impedances of the Slotted Coaxial Lines," *IRE Trans. on Microwave Theory and Techniques* **6 (1958)**, pp. 161 - 166.

[2] Bochenek, K. "Impedanja falowa linii wystepujacej w jednym z rodzajow symetryzatora," *Archiwum Electrotechniki* **5 (1956)**, pp. 135 - 147.

[3] Hilberg, W. **Electrical Characteristics of Transmission Lines.** (Dedham, MA: Artech House Books, 1979), chapter IV.

[4] Rodriguez, David. "Simple Electrostatic Computations for Capacitor Plate Thickness Correction." Private notes, June 1987.

[5] Bottaccini, M.R. **Instruments and Measurements.** (Columbus, OH: Charles E. Merrill Publishing Co., 1975), chapter 3.

[6] Shenfeld, S. **Prediction of Coupling, Shielding, and Grounds For Low-Frequency Fields.** NUSC Report No. 4051; 2 April 1971, p. 110.

[7] Tareev, B. **Physics of Dielectrics.** (Moscow, USSR: Mir Publishers, 1979), pp. 116 - 134.

[8] von Hippel, A.R. **Dielectrics and Waves.** (New York: John Wiley & Sons, 1954), p. 231.

[9] Smolarska, p. 162.

[10] Collin, R.E. "The Characteristic Impedance of a Slotted Coaxial Line," *IRE Trans. on Microwave Theory and Techniques* **4 (1956)**, pp. 4 - 8.

[11] Bochenek, p. 143.

[12] Smolarska, p. 163.

[13] Hilberg, p. 29.

[14] Tareev, p. 120.

[15] Bottaccini, pp. 64 - 67.

[16] Casey, John P. "Effective Dielectric Constant of a Cylindrical Interface," Private communication, July 1988.

[17] King, Ronald W.P., et al. **Antennas in Matter: Fundamentals, Theory, and Applications.** (Cambridge, MA: MIT Press, 1981), pp. 416 - 418.

Bibliography

Abromowitz, M. and I. Stegun, ed. **Handbook of Mathematical Formulas, Graphs, and Mathematical Tables [National Bureau of Standards Applied Mathematics Series, No. 55].** (Washington, D.C.: U.S. Department of Commerce, 1967).

Bochenek, K. "Impedancja folowa linii wystepujacej w jednym z rodzajow symetryzatora." *Archiwum Electrotechniki* **5 (1956)**, pp. 135 - 147.

Bottaccini, M.R. **Instruments and Measurements.** (Columbus, OH: Charles E.Merrill Publishing Co., 1975).

Bowman, F. **Introduction to Elliptic Functions.** (New York: Dover Publications; rpt., 1953).

Brotherton, M. **Capacitors - Their Use in Electronic Circuits.** (Princeton, N.J. :D. Van Nostrand Company, Inc., 1961).

Casey, John P. "Effective Dielectric Constant of a Cylindrical Interface." Private communication, July 1988.

Collin, R.E. "The Characteristic Impedance of a Slotted Coaxial Line." *IRE Trans.on Microwave Theory and Techniques* **4 (1956)**, pp. 4 - 8.

Cooley, William W. "Low-Frequency Shielding Effectiveness of Nonuniform Enclosures." *IEEE Trans. on Electromagnetic Compatibility* **10 (1968)**, pp. 34 - 43.

Fulks, Robert G. and John Lamont. "An Automatic Computer-Controlled System for the measurement of Cable Capacitance." *IEEE Trans. on Instrumentation and Measurement* **17 (1968)**, pp. 299 - 303.

Gebele, Harold W. "Moisture Measurements in Industry." *IRE Trans. on Industrial Electronics* **9 (1962)**, pp. 7 - 10.

Hancock, Harris. **Elliptic Integrals.** (New York: Dover Publications; rpt., 1958).

Hasted, J.B. "The Dielectric Properties of Water ", from **Progress In Dielectrics, vol. 3**, eds. J.B. Birks and J. Hart. (New York: John Wiley and Sons, 1961),.pp. 103 - 149.

Hilberg, Wolfgang. **Electrical Characteristics of Transmission Lines.** (Dedham, MA: Artech House Books, 1979).

Hilberg, Wolfgang. "From Approximations to Exact Relations for Characteristic Impedances." *IEEE Trans. on Microwave Theory and Techniques* **17 (1969)**, pp. 259 - 265.

Hood, J.L.L. "An engineer's log-moisture measurement." *Electronics and Wireless World*, July 1966, pp. 24 - 28.

Jahnke, E. and F. Emde. **Tables of Functions.** (New York: Dover Publications; rpt., 1945).

Joshi, K.K., J.S. Rao and B.N. Das. "Characteristic Impedance of Nonplanar Striplines." *IEE Proc.* **127**, *Pt. H* **(1980)**, pp. 287 - 291.

Keiser, Bernhard. **Principles of Electromagnetic Compatibility, 3rd ed.** (Norwood, MA: Artech House, 1987).

King, Louis V. "Electromagnetic Shielding at Radio Frequencies." *Phil. Mag.* **15 (1933)**, pp. 201 - 223.

King, Ronald W.P., et al. **Antennas in Matter: Fundamentals, Theory, and Applications.** (Cambridge, MA: MIT Press, 1981).

Lin, Weigan. "A Critical Study of the Coaxial Transmission Utilizing Conductors of Both Circular and Square Cross Section." *IEEE Trans. on Microwave Theory and Techniques* **30 (1982)**, pp. 1981 - 1988.

Love, A.E.H. " Some Electrostatic Distributions in Two Dimensions." *Proc. Math. Soc. of London* **22 (1923)**, pp. 337 - 369.

Ott, Henry. **Noise Reduction Techniques in Electronic Systems.** (New York: John Wiley and Sons, 1966).

Palmer, Harlan B. "The Capacitance of a Parallel-Plate Capacitor by the Schwartz-Christoffel Transformation." *Proc. AIEE,* (March 1937), pp. 363 - 366.

Revesz, George. " Capacitive Measurements of High Sensitivity and their applications to Industrial Testing and Control." *IRE Trans. on Industrial Electronics* **3 (1956)**, pp. 32 - 39.

Revesz, George. "Process Instrumentation for the Measurement and Control of Level."*IRE Trans. on Industrial Electronics* **7 (1958)**, pp. 11 - 16.

Rodriguez, David. "Brief Notes on the Static and Dynamic Characteristics of Cable Flooding by Capacitance." NUSC internal memorandum, 23 March 1987.

Rodriguez, David. "Simple Electrostatic Computations for Capacitor Plate Thickness Correction." Private notes, June 1987.

Shenfeld, Saul. **Prediction of Coupling, Shielding, and Grounds For Low-Frequency Fields.** NUSC Report No. 4051, 2 April 1971.

Shenfeld, Saul. "Shielding of Cylindrical Tubes." *IEEE Trans. on Electromagnetic Compatibilty* **10 (1968)**, pp. 29 - 34.

Smolarska, Jadwiga. "Characteristic Impedance of the Slotted Coaxial Line." *IRE Trans. on Microwave Theory and Techniques* **6 (1958)**, pp. 161 - 168.

Stogryn, A. "Equations for calculating the Dielectric Constant of Saline Water." *IEEE Trans. on Microwave Theory and Techniques* **19 (1971)**, pp. 733 - 736.

Tareev, B. **Physics of Dielectrics.** (Moscow, USSR: Mir Publishers, 1979).

Taylor, Leonard S. "Dielectric Properties of Mixtures." *IEEE Trans. on Antennas and Propagation* **13 (1965)**, pp. 943 - 947.

Vokey, David K. "Electronic monitoring system helps combat moisture damage in outside cable plant." *Telephony*, August 10, 1981; pp. 58 - 60, 149.

Von Hippel, Arthur R. **Dielectrics and Waves.** (New York: John Wiley and Sons, 1954).

Wentworth, F.L. and M. Cohn. "Electrical Properties of Sea Ice at 0.1 to 30 Mc/s." *Radio Science* **68D (1964)**, pp. 681 - 691.

Wheeler, Harold A. "Transmission-Line Properties of Parallel Wide Strips by a Conformal-Mapping Approximation." *IEEE Trans. on Microwave Theory andTechniques* **12 (1964)**, pp. 280 - 289.

Wheeler, Harold A. "Transmission-Line Properties of Parallel Strips Separated by a Dielectric Sheet." *IEEE Trans. on Microwave Theory and Techniques* **13 (1965)**, pp.172 - 185.

Wheeler, Harold A. "Transmission-Line Conductors of Various Cross Sections." *IEEE Trans. on Microwave Theory and Techniques* **28 (1980)**, pp. 73 - 83.

INITIAL DISTRIBUTION LIST

Addressee	No. of Copies
SPAWAR PMW-153-2	1
Prof. Rajeev Bansal, Dept. of Electrical and Systems Engineering U-157, University of Connecticut, Storrs, CT 06269	1
Prof. Leo Setian, John Brown University, Box 3058, Siloam Springs, AR 72761	1
Gabriel Silberman, ARDEC, SCMAR-FSP-E, Bldg. 1530, Picatinny Arsenal, Picatinny, NJ 07806-5000	1